Epsilon–optimal synthesis for vehicles with vertically bounded Field-Of-View

Paolo Salaris, Andrea Cristofaro, Lucia Pallottino, Antonio Bicchi

***Abstract*—This paper presents a contribution to the problem of obtaining an optimal synthesis for shortest paths for a unicycle guided by an on–board limited Field–Of–View (FOV) sensor, which must keep a given landmark in sight. Previous works on this subject have provided an optimal synthesis for the case in which the FOV is limited in the horizontal directions (H–FOV, i.e. left and right boundaries). In this paper we study the complementary case in which the FOV is limited only in the vertical direction (V–FOV, i.e. upper and lower boundaries). With respect to the H–FOV case, the vertical limitation is all but a simple extension. Indeed, not only the geometry of extremal arcs is different, but also a more complex structure of the synthesis is revealed by analysis. We will indeed show that there exist initial configurations for which the optimal path does not exist. In such cases, we provide an ε–optimal path whose length approximates arbitrarily well any other shorter path. Finally, we provide a partition of the motion plane in regions such that the optimal or ε–optimal path from each point in that region is univocally determined.**

I. Introduction

The final goal of the proposed research is to study the problem of maintaining visibility of a set of landmarks with a nonholonomic vehicle equipped with a limited Field–Of–View (FOV) sensor. A preliminary analysis on local optimal paths, in case of a set of landmarks and considering a FOV with horizontal bounds, can be found in [1] where a randomized planner is also proposed. To the authors' best knowledge, no results have already been obtained for a FOV with vertical bounds. Hence, in this paper we consider the simplified case of a single landmark determining global optimal paths for a vertically limited FOV. In other words, the goal is to obtain shortest paths from any point on the motion plane to a desired position while keeping, along the path, a given landmark within the vertical bounds of the camera.

Regarding optimal (shortest) paths in absence of sensor constraints, the seminal work on unicycle vehicles [2] provides a characterization of shortest curves for a car with a bounded turning radius. In [3], authors determine a complete finite partition of the motion plane in regions characterizing the shortest path from all points in the same region, i.e. a synthesis. A similar problem with the car moving both forward and backward has been solved in [4] and refined in [5]. The global synthesis for the Reeds and Shepp vehicle has been obtained in [6] combining necessary conditions given by Pontryagin's Maximum Principle (PMP) with Lie algebraic tools. More recently, [7], [8] present time optimal trajectories for differential–drive robots and for nonholonomic bidirectional robots, respectively. Finally, in [9], the minimum wheel rotation problem for differential-drive robots has been solved.

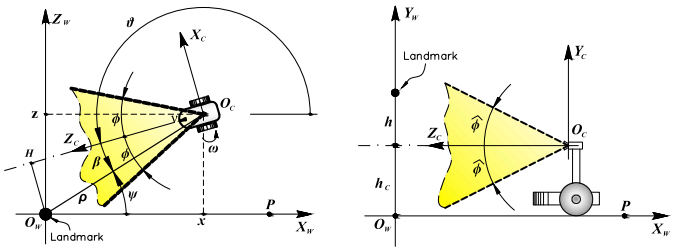

(a) Cartesian and polar coordinates and Horizontal–Field–Of–View (H–FOV) constraints.

(b) Vertical–Field–Of–View (V–FOV) constraints.

Fig. 1. Mobile robot and systems coordinates. The robot's task is to reach P while keeping the landmark within a limited Field–Of–View (dashed lines).

On the other hand, sensor constraints deeply influence the accomplishment of assigned tasks and hence the control laws, especially in those cases in which robots are subject to nonholonomic constraints. Moreover, for self-localization purposes or maintaining visibility of objects in the environment, some landmarks must be kept in sight. In visual servoing tasks, this problem becomes particularly noticeable and in the literature several solutions have been proposed to overcome it, see e.g. [10], [11], [12]. However, the FOV problem has been successfully solved for a unicycle–like vehicle in [13], [14], [15] nevertheless, the resultant path is inefficient and absolutely not optimal. Several preliminary results have been recently obtained in case of navigation in environment with obstacles that may occlude the landmark visibility, see e.g. [16] and [17]. In [17] author propose a motion planning strategy for a humanoid to safely navigate among obstacles while maintaining at least one landmark in sight. The strategy is based on the synthesis in [18] and provides a path that consists of shortest geometric primitives. In [16] necessary and sufficient conditions for the existence of a collision free path that ensure a given landmark visibility also in presence of obstacles are obtained through an iterative algorithm.

A related study, similar to the one analyzed in this paper, has been tackled in [18] where only right and left camera limits, i.e. the Horizontal–FOV (H–FOV) constraints, were taken into account. The camera has been modeled as a frontal and symmetric (with respect to the robot forward direction)

This work was supported by E.C. contracts n.224053 CONET (Cooperating Objects Network of Excellence), n. 257462 HYCON2 (Network of Excellence) and n.2577649 PLANET.

Salaris, Pallottino and Bicchi are with the Research Center "Enrico Piaggio" and Dipartimento di Ingegneria dell'Informazione, University of Pisa, Italy. Bicchi is also with the Department of Advanced Robotics, Istituto Italiano di Tecnologia, Genova, Italy. Cristofaro is with the School of Science and Technology, University of Camerino, Italy.

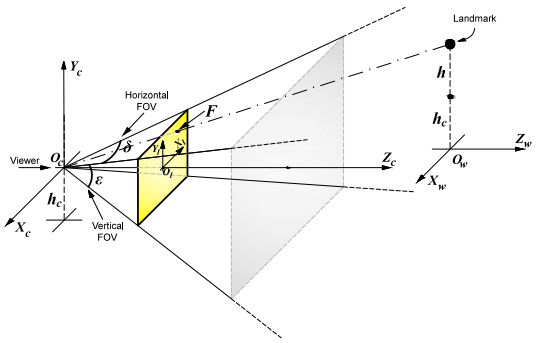

Fig. 2. Sensor model: four-sided right rectangular pyramid.

planar cone, as represented in Fig. 1(a). The constraint on the symmetry (with respect to the robot forward direction) of the planar cone has been relaxed in [19] where the robot forward direction is not necessarily supposed to be included inside the planar cone. After showing that logarithmic spirals, straight lines and rotations on the spot are extremal arcs of the optimal control problem, a finite alphabet of these arcs has been obtained and the shortest paths from any point on the motion plane to a desired final configuration, i.e. a synthesis, has been provided. In [20], based on the geometric properties of the synthesis proposed in [18], optimal feedback control laws which are able to align the vehicle to the shortest path from the current configuration are also defined, for any point on the motion plane. Moreover, based on the same synthesis, a switched, homography–based, visual servoing scheme is proposed in [21] to steer the vehicle along the optimal paths.

However, in real cameras there exist also the upper and lower limits that previous works have not taken into account. Hence, in this work we study the complementary case in which only upper and lower camera limits are considered, i.e. the Vertical–FOV (V–FOV) constraints, see Fig. 1(b). The goal of our research is to obtain first the optimal paths taking into account both kinematics and V–FOV constraints and then the optimal synthesis of the motion plane. Finally, from the optimal synthesis, optimal feedback control laws might be derived to steer the vehicle toward the goal without violating the constraints. Once the synthesis of this problem is obtained, the optimal synthesis for a realistic sensor modeled as a four–sided right rectangular pyramid (see Fig. 2), can be achieved by appropriately merging synthesis provided in [18] with that provided in this paper.

In this work, we first show that involutes of circle, straight lines and rotations on the spot are extremal arcs of the V–FOV problem, and then we exploit geometric properties of these arcs to achieve the synthesis. However, several aspects make the problem addressed in this paper much more difficult with respect to the one in [18] and prevent us to use the same approach to tackle the problem. One is that there exists a compact set around the feature for which paths reaching it now become impracticable since they violate the V–FOV constraints. Moreover, the whole procedure adopted in [18] for obtaining the final synthesis is mainly based on the invariance property of logarithmic spirals with respect to scaling (with center at the origin). Unfortunately, involutes of circle do not have this property and hence a different approach must be used. Moreover, a major challenge is that, for the V–FOV case, there exist points in the motion plane from which the optimal path does not exist. Indeed, the paths would consist of infinite sequences of arcs whose total lengths are anyhow proved to be finite. On the other hand, an ε–optimal path whose length approximates arbitrarily well any other shorter path can be determined and used to obtain an ε–optimal synthesis.

Preliminary results on this problem have been published in [22] where, for space limitations, several proofs and technical details have been omitted. In this paper we briefly report the results in [22] necessary for the characterization of the optimal synthesis together with the missing proofs. From the results in [22] we will characterize the optimal and ε–optimal paths with respect to the relative positions of initial and final points. Finally, we will provide the main contribution of the paper that is the subdivision of the motion plane in regions of points that are characterized by the same optimal or ε–optimal path typology, i.e. the ε–optimal synthesis.

It is worth noticing that the results obtained in this paper are necessary to determine the optimal synthesis for a FOV with both horizontal and vertical limits. This can be done by integrating, with a non straightforward procedure, the obtained synthesis with the one in [18]. Thus, the complete synthesis could be extended to the multi-feature case with the results in [1].

As in previous works, in this paper a fixed on–board camera is considered. There are multiple reasons for our focus on such cameras, of both a technological and a theoretical nature.

From a technological point of view, although pan–tilt cameras costs are not prohibitive, they remain much more complex and prone to failures. Furthermore, angle measurement errors and backlash in the mechanism may add significantly to localization errors. From a functional viewpoint, having a panning mechanism effectively widens the H–FOV by the angular range spanned by the camera motor; similarly, the tilting mechanism widens the V–FOV, which is the issue relevant to this paper. If the pan and tilt angles are wide enough to cover the whole 4π solid angle, then optimal control is trivialized to a non-limited FOV problem. If otherwise the pan/tilt angles are limited (such as e.g. in [16], [1], [17] and [21]), then our problem definition remains valid, only with wider bounds.

From a theoretical point of view, however, our analysis works in the assumption that the camera plane is orthogonal to the motion plane. The control extremals and the synthesis for different tilting angles needs a specific analysis. Moreover, if the tilting angle is changed along the motion, a wholly new optimal control problem with three instead of two inputs is generated. The study of this problem is not considered in this paper.

II. Problem Definition

Consider a vehicle moving on a plane where a right-handed reference frame $\langle W \rangle$ is defined with origin in O_w and axes X_w, Z_w. The configuration of the vehicle is described by $\xi(t) =$

$(x(t), z(t), \theta(t))$, where $(x(t), z(t))$ is the position in $\langle W \rangle$ of a reference point in the vehicle, and $\theta(t)$ is the vehicle heading with respect to the X_w axis (see Fig. 1). We assume that the dynamics of the vehicle are negligible, and that the forward and angular velocities, $v(t)$ and $\omega(t)$ respectively, are the control inputs of the kinematic model of the vehicle. Choosing polar coordinates (see Fig. 1), the kinematic model of the unicycle-like robot is

$$\begin{bmatrix} \dot{\rho} \\ \dot{\psi} \\ \dot{\beta} \end{bmatrix} = \begin{bmatrix} -\cos\beta & 0 \\ \frac{\sin\beta}{\rho} & 0 \\ \frac{\sin\beta}{\rho} & -1 \end{bmatrix} \begin{bmatrix} v \\ \omega \end{bmatrix}. \tag{1}$$

We consider vehicles with bounded velocities which can turn on the spot. In other words, we assume

$$(v, \omega) \in U, \tag{2}$$

where U is a compact and convex subset of $\mathbb{R}^2$, containing the origin in its interior.

The vehicle is equipped with a rigidly fixed pinhole camera with a reference frame $\langle C \rangle = \{O_c, X_c, Y_c, Z_c\}$ such that the optical center O_c corresponds to the robot's center $[x(t), z(t)]^T$ and the optical axis Z_c is aligned with the robot's forward direction. Cameras can be generically modeled as a four-sided right rectangular pyramid, as shown in Fig. 2. Its characteristic solid angle is given by $\Omega = 4\arcsin\left(\sin\hat{\phi}\sin\phi\right)$ and $\varepsilon = 2\hat{\phi}$ and $\delta = 2\phi$ are the apex angles, i.e. dihedral angles measured to the opposite side faces of the pyramid. We will refer to those angles as the vertical and horizontal angular aperture of the sensor, respectively. Moreover, $\hat{\phi}$ is half of the V–FOV angular aperture, whereas ϕ is half of the H–FOV angular aperture.

In [18], authors have provided a complete characterization of shortest paths towards a goal point taking into account only a limited horizontal aperture of the camera and hence modeling the camera FOV as a planar cone moving with the robot. The obtained optimal paths consist of at most 5 arcs of three types: rotations on the spot (denoted by the symbol $*$), straight lines (S) and left and right logarithmic spirals (T^L and T^R). Finally an optimal synthesis has been obtained, i.e. a subdivision of the motion plane in regions such that an optimal sequence of symbols (corresponding to an optimal path) is univocally associated to a region and completely describes the shortest path from each point in that region to the desired goal.

In this paper, we consider only the upper and lower limits of the camera, i.e. we assume $\phi = \pi/2$. Moreover, we consider the most interesting case in which $\hat{\phi}$ is less than $\pi/2$. The goal is hence to obtain the optimal synthesis considering only the V–FOV constraints.

Without loss of generality, the feature to be kept within the vertically limited FOV lays on the axis through the origin O_w, perpendicular to the motion plane (see Fig. 1). Referring to Fig. 2, $h + h_c$ and h are the feature heights from O_w and from the plane $X_c \times Z_c$ respectively. We denote with $(\rho, \psi) = (\rho_P, 0)$ the position, on the X_w axis, of the robot target point P.

Remark 1: In order to maintain the feature within the vertical FOV, the following must hold:

$$\rho\cos\beta \quad \geq \quad \frac{h}{\tan\hat{\phi}} = R_b\,. \tag{3}$$

Indeed, considering a pinhole camera model [23], the position of the landmark in the image plane is given by

$${}^I x = f\frac{{}^c x}{{}^c z}, \tag{4}$$

$${}^I y = f\frac{h}{{}^c z}, \tag{5}$$

where ${}^c x = \rho\sin\beta$ and ${}^c z = \rho\cos\beta$ are the coordinates of the landmark in the camera frame $\langle C \rangle$ and f is the focal length, i.e. $\overline{O_c O_I}$ (see Fig. 2). Since the vehicle is moving on a plane, a constant value of ${}^I y$ corresponds to a constant ${}^c z = \rho\cos\beta$, see Fig. 1(a). The maximum allowable value for ${}^I y$ depends on the vertical angular aperture of the camera, hence ${}^I y \leq f\tan\hat{\phi}$. Finally, substituting ${}^c z = \rho\cos\beta$ in (5) we obtain (3).

Definition 1: Let $Z_0 = \{(\rho, \psi) | \rho < R_b\}$ be the disk centered in the origin with radius R_b and $Z_1 = \{(\rho, \psi) | \rho \geq R_b\}$.

Remark 2: Z_0 is the set of points in $\mathbb{R}^2$ that violates the V–FOV constraint (3) for any value of the bearing angle β. Notice that points with $\rho = R_b$ verify the constraint only if $\beta = 0$. Z_1 is the set of points in $\mathbb{R}^2$ such that inequality (3) holds.

To determine the motion plane synthesis, we are now interested in studying the shortest path covered by the center of the vehicle from any point $Q \in Z_1$ to P, such that the feature is kept in the sensor V–FOV. Hence, the problem is to minimize the cost functional

$$L = \int_0^\tau |v|\,dt\,, \tag{6}$$

under the *feasibility constraints* (2), (3) and the kinematic model (1). Since the cost functional (6) does not weight β the maneuvers consisting of rotations on the spot have zero length. In the following, these zero cost maneuvers, denoted by $*$, will be used only to properly connect other maneuvers, i.e. denoting a non smooth transition.

This problem has been preliminary addressed in [22] where the first step of the characterization of the shortest paths have been considered. However, for space limitations several proofs and results have been omitted. For the sake of clarity and reader convenience, notations, definitions and main results (without proofs) of [22] that are necessary to fully understand the analysis toward the optimal synthesis of the V–FOV, provided in this paper, will be reported.

III. Extremals and optimal concatenations

In this section we briefly characterize the extremals of the optimal control problem, their main geometrical peculiarities and their concatenations that can not be part of optimal paths. Moreover, conditions under which such optimal paths do not exist will also be determined. For those purposes, we start analyzing the V–FOV constraints and the properties of the geometrical curves followed by the vehicle while moving activating the constraints.

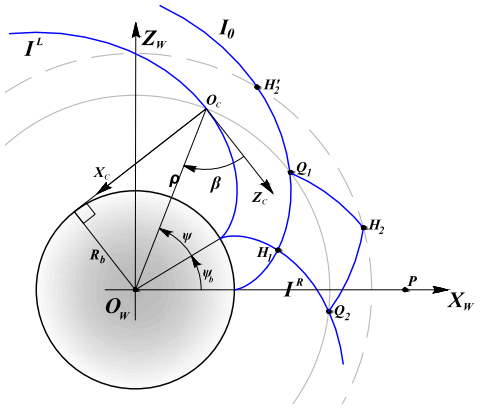

Fig. 3. Extremal arcs for the V–FOV: the involutes of a circle of radius R_b. I_0 is the involute with $\psi_b = 0$. Path $\mathscr{C}_1 = I^{L+} * I^{R-}$ and path $\mathscr{C}_2 = I^{R-} * I^{L+}$ both between Q_1 and Q_2.

The V–FOV constraint is activated for those configurations that verify

$$\rho \cos\beta = R_b. \tag{7}$$

Given the kinematic model of the vehicle, the relationship between the control inputs v and ω required to follow a path along which (7) holds is given by

$$\dot{\rho}\cos\beta - \rho\sin\beta\dot{\beta} = 0 \Rightarrow \rho\sin\beta\,\omega = v.$$

Notice that $\rho\sin\beta$ represents the radius of curvature at a point of the path followed by the vehicle while (7) is satisfied. The trajectory followed with such inputs satisfies $\dot{\psi} = -\tan^2\beta\dot{\beta}$ that by integration gives the following relation between ψ and β,

$$\psi = \psi_b - \tan\beta + \beta. \tag{8}$$

Paths characterized by equations (7) and (8) are curves known as *involutes of a circle*[1] expressed by polar coordinates. ψ_b is the angular coordinate of a point on the involute such that $\beta = 0$, and hence $\rho = R_b$ (see Fig. 3).

To proceed in the analysis, we first need to characterize the geometrical involutes properties and to compute their lengths. First notice that involutes are invariant with respect to rotations (around O_w) and axial symmetries (with the axis through O_w). Hence, for simplicity, we will consider points on the involute given by (7) and (8) with $\psi_b = 0$ and $\beta \in (-\pi/2, 0]$ denoted by I_0.

Remark 3: The relation between ψ and β for points on I_0 is given by the invertible function

$$\Psi(\beta) = \tan\beta - \beta, \qquad \beta \in [0, \frac{\pi}{2}). \tag{9}$$

Its inverse will be denoted by $\Psi^{-1}(\psi)$. Notice that, the function Ψ is increasing and convex for $\beta \in [0, \frac{\pi}{2})$ while the inverse function $\Psi^{-1}(\psi)$ is increasing and concave.

[1]The involute of a circle is the path traced out by a point on a straight line r that rolls around a circle without slipping (see Fig. 3). Notice that, while the vehicle follows an involute of a circle the axis X_c is tangent to the circle with radius R_b and plays the role of r.

Given a point $Q = (\rho_Q, \psi_Q) \in I_0$, the length of the involute arc from Q to $Q_b = (R_b, 0)$ is

$$\ell_0(\beta_Q) = \frac{R_b}{2\cos^2(\beta_Q)} - \frac{R_b}{2}. \tag{10}$$

Given two points Q_1 and Q_2 on I_0 with $\rho_{Q_1} \geq \rho_{Q_2}$ the length of the involute arc between the points is

$$\ell(Q_2, Q_1) = \ell_0(\beta_{Q_2}) - \ell_0(\beta_{Q_1}). \tag{11}$$

where β_i and ψ_i are given by equations (7) and (9) respectively.

A. V–FOV Extremals

For any point on circumference C_{R_b} with radius R_b and centered in O_w there are two involutes of circle rotating clockwise and counterclockwise. We refer to these two involutes as *Left* and *Right*, and by symbols I^L and I^R, respectively (see Fig. 3). The adjectives "Left" and "Right" indicate the half-plane where the involute starts for an on-board observer aiming at the landmark.

Following the same Hamiltonian-based approach used in [18], the extremal arcs (i.e. curves that satisfy necessary conditions for optimality, see [24]) are the involutes I^R and I^L, the turn on the spot $*$ and the straight lines S. Moreover, as extremal arcs can be executed by the vehicle in either forward or backward direction, superscripts $+$ and $-$ will be used in the following in order to make this explicit. As a consequence, extremal paths consist of sequences, or *words*, comprised of symbols in the finite alphabet $\mathscr{A} = \{*, S^+, S^-, I^{R+}, I^{R-}, I^{L+}, I^{L-}\}$. The set of possible words generated by the symbols in $\mathscr{A}$ is a language $\mathscr{L}$.

B. Optimal concatenation of extremals

Let $\mathscr{P}_Q$ be the set of all feasible extremal paths from Q to P. We now exploit the particular symmetries of the considered problem to determine extremals concatenations that do not belong to the optimal path in $\mathscr{P}_Q$. For example, the analysis of optimal paths in $\mathscr{P}_Q$ can be done considering only the upper half plane with respect to the X_w axis. The optimal synthesis for the lower half plane can be obtained by replacing $+$ $(-)$ with $-$ $(+)$ and R (L) with L (R).

Definition 2: A path in $\mathscr{P}_Q$ (i.e. from Q to P), consisting of a sequence $w \in \mathscr{L}$ of symbols in $\mathscr{A}$, is a *palindrome symmetric path* if w is palindrome and the path is symmetric with respect to the bisectrix of angle $\widehat{QO_WP}$.

We recall that a word is palindrome if it reads equally forward or backward. As an example, the path $S^+I^{L+} * I^{R-}S^-$ is a palindrome symmetric path, associated to the palindrome word *SIIS*, if the straight arcs and the involute arcs are of equal length pairwise.

Proposition 1: For any path in $\mathscr{P}_Q$ with $\rho_Q = \rho_P$ there always exists a palindrome symmetric path in $\mathscr{P}_Q$ whose length is shorter or equal.

The proof of this proposition can be found in [22].

Before determining the extremals concatenations that characterize the optimal paths, we start considering the regions of points from which P can be reached with extremals S^+ or S^-.

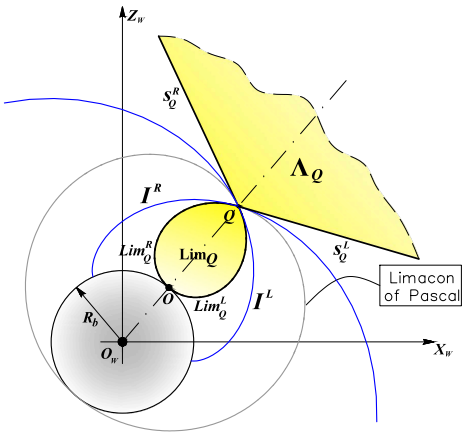

Fig. 4. Region Lim_Q with its border $\partial Lim_Q = Lim_Q^R \cup Lim_Q^L$ and cone Λ_Q delimited by half–lines s_Q^R and s_Q^L.

We will show such regions are closed with borders described by half–lines and curves known as Pascal's Limaçons, [25]

Definition 3: For a point $Q \in \mathbb{R}^2$, Lim_Q^R (Lim_Q^L) denotes the arc of the Pascal's Limaçon from Q to O such that, $\forall V \in Lim_Q^R$ (Lim_Q^L), $\widehat{QVO_w} = \pi - \tilde{\beta}$, with $\tilde{\beta} = \arctan\left(\frac{\rho_Q}{Rb}\sin\beta\right)$, in the half-plane on the right (left) of $\overline{QO}_w$ (cf. Fig. 4). Also, let Lim_Q be the region with borders Lim_Q^R and Lim_Q^L from Q to O.

Definition 4: For a point $Q \in \mathbb{R}^2$, s_Q^R (s_Q^L) denotes the half-line from Q forming an angle $\psi_Q + \tilde{\beta}$ ($\psi_Q - \tilde{\beta}$), where $\tilde{\beta} = \arccos\left(\frac{R_b}{\rho_Q}\right)$, with the X_w axis (cf. Fig. 4). Also, let Λ_Q be the cone delimited by s_Q^R and s_Q^L.

Proposition 2: For any starting point Q, all points of Lim_Q (Λ_Q) are reachable by a forward (backward) straight path without violating the V–FOV constraints.

The proof of Proposition 2 (that has been omitted in [22] for space limitations), is based on how the projection on the image plane of the landmark moves within the sensor limits (see [26]) when vehicle performs extremal maneuvers and is reported in Appendix A.

At this point the regions associated to the single straight line maneuvers have been obtained. Following a similar approach to the one used in [18], the goal is to obtain a sufficient family of optimal paths from which the complete synthesis can be obtained. Unfortunately, in this case optimal paths do not always exist as stated in the following theorem.

Theorem 1: For any Q on the upper half plane, one of the following conditions is verified.

1) There exists a shortest path toward P of type $S^+I^{L+} * I^{R-}S^-$ or $I^{R-} * I^{L+}$ (or degenerate cases, with sub–paths of zero length, e.g. $S^+ * S^-$).
2) The infimum of the cost functional L is not reached and hence the shortest path does not exist.

In order to prove Theorem 1 we proceed showing that particular extremals concatenations can not belong to any optimal path. In [22] some results have been obtained in this direction and are summarized in the following Remark for reader convenience.

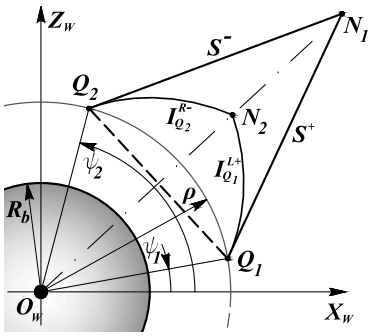

Fig. 5. Path of type $S_{Q_2}^- * S_{Q_1}^+$ from $Q_2 = (\rho, \psi_2)$ to $Q_1 = (\rho, \psi_1)$ with $\psi_2 > \psi_1$ can be shortened by a path of type $I_{Q_2}^{R-} * I_{Q_1}^{L+}$ (see Proposition 3).

Remark 4: For symmetry properties, it is sufficient to consider a starting point $Q = (\rho_Q, \psi_Q)$ with $\psi_Q \geq 0$. From such Q the optimal path toward P lays on the upper half-plane and arcs of type I^{R+} and I^{L-} are not part of the optimal path. Moreover, in the optimal paths the arc S^- can not be followed by arcs of type I^{R-} and I^{L+} while arc S^+ can not follow arcs of type I^{L+} and I^{R-}.

Those results can be further refined with the following proposition that excludes concatenations of type $S^- * S^+$ from optimal paths.

Proposition 3: Any path of type $S^- * S^+$ between $Q_1 = (\rho, \psi_1)$ and $Q_2 = (\rho, \psi_2)$ with $\psi_2 > \psi_1$ can be shortened by a path of type $I^{R-} * I^{L+}$.

Proof: Referring to Fig. 5, let N_1 be the switching point between arcs S^- and S^+. From Proposition 2 we have that $N_1 \in \Lambda_{Q_2} \cap \Lambda_{Q_1}$. However, among all paths of type $S^- * S^+$, the shortest one has $N_1 \in \partial\Lambda_{Q_2} \cap \partial\Lambda_{Q_1}$. In this case, from Definition 4, $I_{Q_2}^{R-}$ is tangent to S^- in Q_2 and $I_{Q_1}^{L+}$ is tangent to S^+ in Q_1. Moreover, the path $I^{R-} * I^{L+}$ lays between $S^- * S^+$ and $\overline{Q_1Q_2}$. For the convexity of both paths, the length of $S^- * S^+$ is longer than the length of $I^{R-} * I^{L+}$ and hence the thesis. ■

Extremals can be represented by nodes of a graph while possible concatenation by arrows where an arc with $(*)$ denotes a non smooth concatenation. The graph reported in Fig. 6 represent a graphical summary of the results obtained so far. The obtained graph is not acyclic and hence optimal

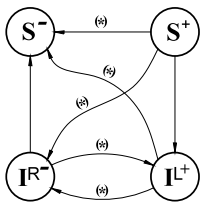

Fig. 6. Extremals and sequences of extremals from points $\mathbb{R}^2$.

path consisting of infinite number of extremals are, at this

point, neither excluded nor proved. Hence, to conclude the analysis of optimal extremal concatenations we need to study concatenations of type $I^{L+} * I^{R-}$ and $I^{R-} * I^{L+}$.

IV. Infinite sequences of involute arcs

In this section we will show that the particular characteristics of the involute arcs may give rise to an infimum (and finite) arc length consisting of infinite involutes of infinitesimal length. To study the occurrence of such peculiarity, we consider $Q_1 = (\rho_{Q_1}, \psi_{Q_1})$ and $Q_2 = (\rho_{Q_2}, \psi_{Q_2})$ with $\rho_{Q_1} = \rho_{Q_2}$ and $\psi_{Q_1} > \psi_{Q_2}$. The points Q_1 and Q_2 can be connected by two paths, each one palindrome and hence symmetric with respect to the bisectrix of angle $\widehat{Q_1 O_w Q_2}$, consisting of two pairs of involute curves $\mathscr{C}_1 = I^{L+} * I^{R-}$ and $\mathscr{C}_2 = I^{R-} * I^{L+}$. Let $H_1 = (\rho_{H_1}, \psi_{H_1})$ and $H_2 = (\rho_{H_2}, \psi_{H_2})$ be the points of intersection of the involute curves on $\mathscr{C}_1$ and $\mathscr{C}_2$ respectively, i.e. $\rho_{H_1} < \rho_{Q_i} < \rho_{H_2}$ and $\psi_{H_1} = \psi_{H_2}$. We denote by $L(\mathscr{C}_1)$ and $L(\mathscr{C}_2)$ the lengths of the curves $\mathscr{C}_1$ and $\mathscr{C}_2$, respectively.

The goal of this section is to prove that the shortest path consisting only of involutes, between two points Q_1 and Q_2 on a circumference, is of type $\mathscr{C}_2$ (evolving outside the circumference) if ρ_{Q_1} and the angle $\widehat{Q_1 O_w Q_2}$ are sufficiently small. On the other hand, it is of type $\mathscr{C}_1$ (hence a pair of involute evolving inside the circumference) if ρ_{Q_1} is sufficiently large while the angle $\widehat{Q_1 O_w Q_2}$ is sufficiently small. Otherwise, the shortest path consisting only of involutes does not exist. More formally, we will prove

Theorem 2: Given the points $Q_1 = (\rho_{Q_1}, \psi_{Q_1})$ and $Q_2 = (\rho_{Q_2}, \psi_{Q_2})$ with $\rho_{Q_1} = \rho_{Q_2}$ and $\psi_{Q_1} > \psi_{Q_2}$. Recalling that $\rho_2 = \sqrt{2} R_b$, it holds that

1) for $\rho_{Q_1} \in [R_b, \rho_2)$,
   a) if $\psi_{Q_1} - \psi_{Q_2} \leq 2(\Psi(\pi/4) - \psi_{Q_1})$ the optimal trajectory from Q_1 to Q_2 is $\mathscr{C}_2 = I^{R-} * I^{L+}$.
   b) $\psi_{Q_1} - \psi_{Q_2} > 2(\Psi(\pi/4) - \psi_{Q_1})$ the shortest path does not exist.
2) For $\rho_{Q_1} \geq \rho_2$
   a) if $\psi_{Q_1} - \psi_{Q_2} > 2(\psi_{Q_1} - \Psi(\pi/4))$ the shortest path does not exist.
   b) if $\psi_{Q_1} - \psi_{Q_2} \leq 2(\psi_{Q_1} - \Psi(\pi/4))$ the optimal trajectory from Q_1 to Q_2 is $\mathscr{C}_1 = I^{L+} * I^{R-}$

The proof of this theorem follows straightforwardly from the results stated in the following two propositions. In the first one only pairs of involutes ($\mathscr{C}_1$ and $\mathscr{C}_2$) are taken into account while in the second an arbitrary number of involutes are considered. Hence, we start comparing the lengths $L(\mathscr{C}_1)$ and $L(\mathscr{C}_2)$ to characterize the conditions on ρ_{Q_1} and ρ_{H_1} under which one is smaller than the other.

Proposition 4: There exist $\bar{\rho}$ and $\tilde{\rho}$ with $\bar{\rho} > \rho_2 > \tilde{\rho}$ such that

1) $\rho_{Q_1} \leq \rho_2 \Rightarrow L(\mathscr{C}_2) \leq L(\mathscr{C}_1) \; \forall \rho_{H_1}$.
2) $\rho_{Q_1} \in (\rho_2, \bar{\rho}), \rho_{H_1} < \tilde{\rho} \Rightarrow L(\mathscr{C}_2) < L(\mathscr{C}_1)$
3) $\rho_{Q_1} \in (\rho_2, \bar{\rho}), \rho_{H_1} > \tilde{\rho} \Rightarrow L(\mathscr{C}_1) < L(\mathscr{C}_2)$
4) $\rho_{Q_1} \geq \bar{\rho} \Rightarrow L(\mathscr{C}_1) \leq L(\mathscr{C}_2) \; \forall \rho_{H_1}$.

The proof of this proposition, omitted in [22] for brevity, can be found in Appendix B. The value ρ_{H_1} of the switching point H_1 with respect to $\tilde{\rho}$ can be rewritten in terms of the angle $\psi_{Q_1} - \psi_{Q_2}$ spanned by $\mathscr{C}_1$ and $\mathscr{C}_2$ as in the following proposition where we consider also the possibility of connecting Q_1 and Q_2 with path consisting of an arbitrary number of involutes.

The following Proposition is a collection of results in [22] and provides conditions under which the optimal path does not exist.

Proposition 5: Consider the points $Q_1 = (\rho_{Q_1}, \psi_{Q_1})$ and $Q_2 = (\rho_{Q_1}, \psi_{Q_2})$ with $\psi_{Q_1} > \psi_{Q_2}$.

1) if $\rho_{Q_1} < \rho_2$, and $\Psi(\pi/4) - \psi_{Q_1} \geq \frac{\psi_{Q_1} - \psi_{Q_2}}{2}$ the optimal trajectory consisting of involutes from Q_1 to Q_2 is $\mathscr{C}_2 = I^{R-} * I^{L+}$.
2) if $\rho_{Q_1} = \rho_2$ and $\forall \psi_{Q_2}$, the optimal (shortest) path between Q_1 and Q_2 consisting of involutes does not exist, i.e. the infimum of the cost functional (6) is not reached.
3) If $\rho_{Q_1} > \rho_2$, and $\psi_{Q_1} - \Psi(\pi/4) \geq \frac{\psi_{Q_1} - \psi_{Q_2}}{2}$ the optimal trajectory consisting of involutes from Q_1 to Q_2 is $\mathscr{C}_1 = I^{L+} * I^{R-}$.

The proposition states that whenever $\mathscr{C}_1$ or $\mathscr{C}_2$ intersects the circumference of radius ρ_2 they can both be shortened. For example, if $\mathscr{C}_1$ crosses the circumference of radius ρ_2 in G_1 and G_2 the sub–path between such points can be shortened with a path of type $\mathscr{C}_2$ (see Proposition 4 second item). Moreover, from Proposition 4 third item, this shorter path of type $\mathscr{C}_2$ can in turn be shortened by a path consisting of two or more sub–paths of type $\mathscr{C}_2$. By iterating this procedure it is possible to conclude the non-existence of a shortest path between Q_1 and Q_2 with $\rho_{Q_1} = \rho_{Q_2} = \rho_2$.

For those cases in which the path does not exist, we are now interested in the infimum of the lengths of the paths consisting of infinite pairs of involutes of type $\mathscr{C}_2$. The following Theorem, whose proof can be found in [22], states that such infimum length is finite.

Theorem 3: Consider $\rho = \rho_2$, the point $Q_1 = (\rho, \psi_{Q_1}) \in I_0$ and a point $Q_2 = (\rho, \psi_{Q_2})$ with $\psi_{Q_1} > \psi_{Q_2}$ and $\psi_{Q_1} - \psi_{Q_2} \leq \pi$. The infimum of the lengths of the paths consisting of infinite sub–paths of type $\mathscr{C}_2$ from Q_1 to Q_2 is finite and

$$L_{inf}(Q_1, Q_2) = \sqrt{2}(\rho_2(\psi_{Q_1} - \psi_{Q_2}))$$

i.e. $\sqrt{2}$ times the length of the circular arc from Q_1 to Q_2 on the circumference with radius ρ_2.

From a practical point of view, the infimum length path can be approximated by paths consisting of a finite sequence of involutes. The approximation error is as smaller as more accurate is the wheel motor.

Definition 5: $C^{(n)}$ is the path from Q_1 to Q_2 on the circumference of radius ρ_2 consisting of n identical sub–paths of type $\mathscr{C}_2$, i.e. $C^{(n)} = I^{R-} * I^{L+} * I^{R-} * I^{L+} * \cdots * I^{R-} * I^{L+} * I^{R-} * I^{L+}$.

The following corollary provides a sufficient number n of sub–paths of type $\mathscr{C}_2$ in $C^{(n)}$ such that the length of any other shorter path is no longer than an arbitrarily small $\varepsilon > 0$.

Corollary 1: Given a trajectory $C^{(n)}$ from Q_1 to Q_2 on the circumference of radius ρ_2 and a positive parameter $\varepsilon > 0$, there exists $c_0 > 4R_b$ such that for

$$n \geq \frac{c_0(\psi_{Q_1} - \psi_{Q_2})^2}{2\varepsilon}$$

we have $L(C^{(n)}) - L_{inf}(Q_1, Q_2) \leq \varepsilon$.
The proof can be found in Appendix C.

From a practical point of view, consider a robot whose motor accuracy allows it to follow a path of type $\mathscr{C}_2$ on the circumference of radius ρ_2 with amplitudes larger than δ. Hence, given points Q_1 to Q_2 on the circumference of radius ρ_2, the path of minimum length that can be followed by the robot is $C^{(n)}$ with $n = \lfloor \frac{|\psi_{Q_2} - \psi_{Q_1}|}{\delta} \rfloor$ whose length can be computed and compared with L_{inf}.

Definition 6: Given $\varepsilon > 0$, $Z_\varepsilon = C^{(n(\varepsilon))}$ is the path consisting of a sequence of $n(\varepsilon)$ arcs of type $\mathscr{C}_2$ on circumference of radius ρ_2.

Since the infimum length is finite and there exist arcs of type Z_ε whose lengths are arbitrarily close to the infimum one, with an abuse of notation we will denote with Z the non existing but approximable path and we consider Z as a pseudo extremal arc. The alphabet $\mathscr{A}$ is extended with Z obtaining a new alphabet $\mathscr{A}_Z$. If a path contains the symbol Z we use the analytical expression of the path length to determine the *infimum length path* from any point of the motion plane. Notice that such paths are optimal only if they do not contain arcs Z. With a slight abuse of language sequences associated to infimum length paths will be referred to as the optimal language on $\mathscr{A}_Z$ and the induced synthesis will be referred to as optimal synthesis. True ε–optimal synthesis will finally be obtained substituting Z with its ε–optimal subpath Z_ε.

V. The optimal language

Based on the results of previous sections we are now interested in determining the optimal language that characterizes the infimum length paths. Based on Theorem 2, it follows that sequences $S^+ * I^{R-}$ and $I^{L+} * S^-$ do not belong to any infimum length path. Indeed it holds

Proposition 6: Any path of type $S^+ * I^{R-}$ or $I^{L+} * S^-$ can be shortened by a path of type $S^+ I^{L+} * I^{R-} S^-$ or $S^+ I^{L+} * Z * I^{R-} S^-$.

The proof of this proposition can be found in Appendix D. As a consequence, the so called optimal language $\mathscr{L}_Z$ can be described by the graph in Fig. 7.

The symbol Z occurs at most once in infimum length paths as a consequence of the following Proposition.

Proposition 7: For any pair of points Q_1 and Q_2 with $\rho_{Q_1} = \rho_{Q_2} = \rho_2$, the path of infimum length from Q_1 to Q_2 is Z.

Proof: From the graph in Fig. 7 the only possible way to connect Q_1 and Q_2 is with paths of type Z or with concatenations of type $S^+ * I^{R-}$ and $I^{L+} * S^-$. From the proof of Proposition 6 such concatenation can be shortened by paths of type $I^{L+} * I^{R-}$ that in turn can be shortened by Z (see point 2 of Proposition 5). ■

We are finally able to prove Theorem 1 that can now be refined with the inclusion of the infimum length arc Z.

Theorem 1: For any Q on the upper half plane, one of the following conditions is verified.

1) There exists a shortest path toward P of type $S^+ I^{L+} * I^{R-} S^-$ or $I^{R-} * I^{L+}$ (or degenerate cases, with sub–paths of zero length, e.g. $S^+ * S^-$).

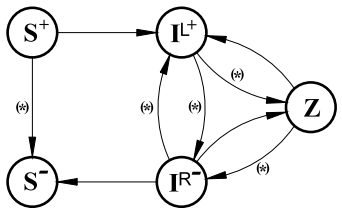

Fig. 7. Extremals in $\mathscr{A}_Z$ and sequences of extremals (in the optimal language) from points in $\mathbb{R}^2$. Notice that in optimal paths the switching between involutes may occur only once, e.g. $I^{L+} * I^{R-} * I^{L+}$ is never optimal. Moreover, the symbol Z may appear only once in sequences associated to infimum length paths.

2) The infimum of the cost functional L is not reached and hence the shortest path does not exist. Considering the infimum arc Z the infimum length paths are of type $S^+ I^{L+} * Z * I^{R-} S^-$, $S^+ I^{L+} * Z I^{L+}$, $I^{R-} Z * I^{R-} * S^-$ or $I^{R-} Z I^{L+}$ (or degenerate cases).

Proof: From previous results, the optimal language represented in Fig. 7 has been obtained. Moreover, as a consequence of Proposition 7, symbol Z may appear only once in infimum length paths. On the other hand, sequences of three or more involutes are never optimal. Indeed, one of the two concatenations $I^{L+} * I^{R-}$ and $I^{R-} * I^{L+}$ can always be shortened. Which is the concatenation that can be shortened depends on their evolution with respect to C_2. For example, when evolving inside C_2, $I^{L+} * I^{R-}$ is longer than a path of type $I^{R-} * I^{L+}$ or $I^{R-} Z I^{L+}$. Finally, sequences of type $Z I^{L+} * I^{R-}$ and $Z * I^{R-} * I^{L+}$ are never part of an infimum length path. Indeed, the subpath $I^{L+} * I^{R-}$ ($I^{R-} * I^{L+}$) after Z evolves outside (inside) C_2 and hence can be shortened. Similarly, paths of type $I^{R-} * I^{L+} * Z$ and $I^{L+} * I^{R-} Z$ are never part of an infimum length path. Hence the thesis.

■

VI. V–FOV Optimal Synthesis

In this section we analyze the length of the extremal paths from any point of the motion plane considering the alphabet $\mathscr{A}_Z$.

Based on all previous results, circumference C_2 of radius $\rho_2 = R_b\sqrt{2}$ plays an important role and the resulting optimal synthesis deeply depends on the position of the desired and initial points $P = (\rho_P, 0)$ and $Q = (\rho_Q, \psi_Q)$, respectively, with respect to C_2. For this reason, to simplify the analysis, the optimal graph represented in Fig. 7 will be specialized depending on where Q and P are with respect to C_2. Notice that for all the positions of Q, P and C_2 there are at most 4 switching among extremals that are summarized in the following theorem that corresponds to a detailed version of Theorem 1. Indeed, Theorem 4 specifies the infimum path length type depending on the values of ρ_Q, ρ_P and ρ_2.

Theorem 4: Given the initial point $Q = (\rho_Q, \psi_Q)$, the final point $P = (\rho_P, 0)$ and the circumference C_2 of radius ρ_2, the optimal language $\mathscr{L}_O$ is characterized as follows:

a) For $\rho_Q, \rho_P \leq \rho_2$ the infimum length paths are of type $S^+ I^{L+}$, $I^{R-} S^-$, $I^{R-} * I^{L+}$ or $I^{R-} Z * I^{L+}$ (or degenerate cases).

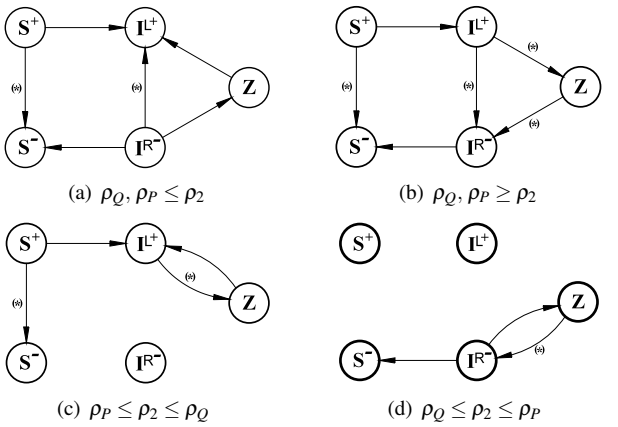

(a) $\rho_Q, \rho_P \leq \rho_2$ (b) $\rho_Q, \rho_P \geq \rho_2$

(c) $\rho_P \leq \rho_2 \leq \rho_Q$ (d) $\rho_Q \leq \rho_2 \leq \rho_P$

Fig. 8. Extremals and sequences of extremals, forming the sufficient ε–optimal language depending on the values of ρ_P and ρ_Q with respect to ρ_2. The symbol Z may appear only once in sequences associated to infimum length paths.

b) For $\rho_Q, \rho_P \geq \rho_2$ the infimum length paths are of type $S^+I^{L+} * I^{R-}S^-$ or $S^+I^{L+} * Z * I^{R-}S^-$ (or degenerate cases).
c) For $\rho_P \leq \rho_2 \leq \rho_Q$ the infimum length paths are of type S^+I^{L+} or $S^+I^{L+} * ZI^{L+}$ (or degenerate cases).
d) For $\rho_Q \leq \rho_2 \leq \rho_P$ the infimum length paths are of type $I^{R-}S^-$ or $I^{R-}Z * I^{R-}S^-$ (or degenerate cases).

The result of the theorem is summarized in Fig. 8 while its proof can be found in Appendix E. Given the deep differences of the obtained optimal languages, next subsections are dedicated to determine the optimal synthesis depending on the position of final point P with respect to C_2.

A. Optimal synthesis for P with $\rho_P \leq \rho_2$

Consider the partition of the upper half–plane in eight regions illustrated in Fig. 9. Regions are generalized polygonals characterized by vertices and whose boundaries belong either to the extremal curves or to the switching loci. Such regions characterize the optimal synthesis as stated in the following theorem that summarizes one of the main contributions of this paper.

Theorem 5: The synthesis of the upper half–plane taking into account the infimum path length Z as an extremal, is described in Fig. 9 and Table I. For each region, the associated path type entirely defines a path of infimum length to the goal.

To simplify the proof of this theorem we first need to analyze two cases corresponding to initial point Q inside or outside C_2.

Referring to the graph in Fig. 8(a), we start considering initial point Q with $\rho_Q \leq \rho_2$. Let P_2 be the intersection point of C_2 with I_P^L, see Fig. 9.

Proposition 8: Given $Q \in C_2 \setminus \Lambda_P$ the infimum path length is given by a path of type ZI_P^{L+} if $\psi_Q \geq \psi_{P_2}$, and of type $S^+I_P^{L+}$ otherwise. The degenerate case S^+ occurs for $Q \in C_2 \cap \Lambda_P$.

Proof: The simple case of the minimum path length of type S^+ when $Q \in C_2 \cap \Lambda_P$ follows from Proposition 2. Consider now $Q \in C_2 \setminus \Lambda_P$, path $S^+I_P^{L+}$ exists only if Q is such that $Lim_Q \cap I_P^{L+} \neq \emptyset$ and, in this case, the switching point $V \in Lim_Q^L \cap I_P^{L+}$. Hence, until ψ_Q is smaller than ψ_{P_2} it holds $Lim_Q \cap I_P^{L+} \neq \emptyset$, and the optimal path is of type $S^+I_P^{L+}$. As soon as ψ_Q becomes larger than ψ_{P_2} we have $Lim_Q \cap I_P^{L+} = \emptyset$ and hence, from Proposition 7, the only admissible way to reach the involute I_P^{L+} from Q is towards Z. ■

Region	Included Vertices	Included Boundaries	Optimal Path Type
I	O, P	Lim_P^R	S^-
I_C	P	s_P^R	S^+
II	P	C_{R_b}, Lim_P^R, I_P^R	$I^{R-}S^-$
II_C	P	s_P^R, I_P^L, $s_{P_5}^R$	S^+I^{L+}
III	P, P_2	C_{R_b}, I_P^L, I_P^R, $I_{P_2}^L$	$I^{R-}I_P^{L+}$
IV	P_2	C_{R_b}, $I_{P_2}^L$, C_2	$I^{R-}ZI_P^{L+}$
V	P_2, P_5	$I_{P_2}^L$, C_2, C_5	$I^{L+} * ZI_P^{L+}$
VI	P_5	C_5, $s_{P_5}^R$	$S^+I^{L+} * ZI_P^{L+}$

TABLE I. OPTIMAL SYNTHESIS IN THE UPPER HALF–PLANE WHEN $\rho_P \leq \rho_2$. C_5 IS THE CIRCUMFERENCE OF RADIUS $\rho_5 = \sqrt{5}R_b$ AND $P_5 \equiv C_5 \cap I_P^L$ WHILE $P_2 \equiv C_2 \cap I_P^L$.

Referring to the graph in Fig. 8(c), we now consider initial point Q with $\rho_Q \geq \rho_2$.

Proposition 9: Given Q on I_P^L, the infimum length paths from Q to P are of type I_P^{L+} if $\beta_Q \leq \arctan(2)$ (i.e. $\rho_Q \leq \rho_5 = R_b\sqrt{5}$) and of type $S^+I^{L+} * ZI_P^{L+}$ otherwise. The locus of switching points between S^+ and I^{L+} is the circumference C_5 centered in the origin with radius ρ_5.

Proof: Consider a point Q with $\rho_Q > \rho_2$ on I_P^L. Referring to the graph in Fig. 8(c), the path from Q to P is of type $S^+I^{L+} * ZI_P^{L+}$. All those paths go through the intersection point P_2 between I_P^{L+} and C_2 (see Fig. 9) toward P. Hence, we may consider only the sub–path $S^+I^{L+} * Z$ from Q to P_2.

Let V and N be the switching points between the straight line and the involute and between the involute and Z, respectively. The straight sub–path S^+ from Q can be parametrized by the bearing angle $\beta_S \in [0, \beta_Q]$ in Q where $\beta_Q = \arccos\left(\frac{R_b}{\rho_Q}\right)$ is the bearing angle of the vehicle aligned with I^{L+} in Q. The switching point V lays on Lim_Q^L and hence S^+ is tangent in V to an involute. Hence, the bearing angle in V is (cf. proof of Proposition 2)

$$\beta_V = \arctan\left(\frac{R_b}{\rho_Q}\sin\beta_S\right) = \arctan\left(\frac{\sin\beta_S}{\cos\beta_Q}\right). \qquad (12)$$

The length of the considered sub–path $S_Q^+I^{L+} * Z$ from Q to P_2 is given by $L = l_S + l_I + l_Z$. From the equation of the Pascal's Limaçon reported in the proof of Proposition 2 the length of the straight arc is

$$l_S = R_b\left(\frac{\cos\beta_S}{\cos\beta_Q} - 1\right). \qquad (13)$$

From (10) the length of the involute arc is

$$l_I = \ell(V, N) = \ell_0(\beta_V) - \ell_0(\beta_N). \qquad (14)$$

Finally, from Theorem 3

$$l_Z = 2R_b\left(\Psi(\beta_Q) - \Psi(\beta_V) - \beta_V + \beta_S\right). \qquad (15)$$

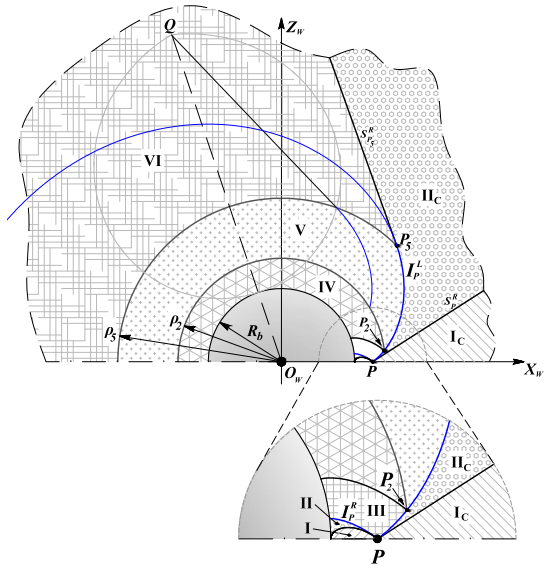

Fig. 9. Optimal synthesis with $R_b \leq \rho_P \leq \rho_2$.

From (9), (10) and (12) the derivative of L with respect to β_S is given by

$$\frac{\partial L(\beta_S)}{\partial \beta_S} = R_b \left(-1+\frac{\cos\beta_S}{\cos\beta_Q}\right)\left(-2+\frac{\sin\beta_S}{\cos\beta_Q}\right),$$

that is zero if $\beta_S = \beta_Q$ and if $\beta_S = \arcsin(2\cos\beta_Q)$ with $\beta_Q \geq \arctan(2)$ (to ensure $\beta_S \leq \beta_Q$).

Notice that if $\beta_Q \leq \arctan(2)$ the length is decreasing and hence the minimum is attained at $\beta_S = \beta_Q$ (that corresponds to a zero length S and Z and an optimal path from Q to P of type I^+_P), for $\beta_Q \geq \arctan(2)$ the minimum is attained with $\beta_S = \arcsin(2\cos\beta_Q)$ (that corresponds to an optimal path from Q to P of type $S^+I^{L+} * ZI^{L+}_P$). Considering the optimal value $\beta_S = \arcsin(2\cos\beta_Q)$, the corresponding point V has bearing angle $\beta_V = \arctan(2)$ and it does not depend on β_Q. Indeed, the locus of switching points V is the circumference C_5 centered in the origin and with radius $\rho_5 = R_b\sqrt{5}$. ■

To prove Theorem 5 we now study each region separately. Regions are defined in Table I and represented in Fig. 9.

Proof: (Theorem 5)

Region I, I_C: From any point in this region it is possible to reach P with a straight path in backward (Region I) or forward (Region I_C) motion without violating the V–FOV constraint (cf. Proposition 2).

Region II: For any Q in this region it holds $\rho_Q \leq \rho_P$. From any of those Q, P cannot be reached with only a straight line or only an involute covered backward. Moreover, the involute I^R_Q intersects Lim_P before than intersecting the involute I^{L+}_P or C_2, i.e. extremal I^{R-}_Q cannot be followed neither by I^{L+}_P nor by Z. Hence, referring to the graph in Fig. 8(a), the only possible path from Q to P is $I^{R-}_Q S^-_P$.

Region III: From any Q in this region the point P cannot be reached with only a straight line or only an involute covered backward. Moreover, the involute I^R_Q intersects I^{L+}_P before intersecting C_2 and does not intersect Lim_P, i.e. extremal I^{R-}_Q cannot be followed neither by Z nor by S^-. Hence, the only possible concatenation is $I^{R-}_Q * I^{L+}_P$, see Fig. 8(a).

Region IV: For any Q in this region it holds $\rho_Q \leq \rho_P$. From any Q, referring to graph in Fig. 8(a), the only possible path toward P is $I^{R-}_Q Z I^{L+}_P$. Indeed, P cannot be reached with only a straight line or only an involute covered backward. Moreover, the involute I^R_Q intersects C_2 before than I^L_P and does not intersect Lim_P, i.e. I^{R-}_Q can not be followed by S^- or by I^{L+}.

Region V: From Proposition 9, since the region is delimited by C_5, the infimum length path is of type $I^{L+} * ZI^{L+}_P$.

Region VI: We start considering Q in the area delimited by C_5 and the involute I^L_P starting from point P_5. From Proposition 9, for such Q there exists an infimum length path toward P from a point on I^L_P that crosses Q. Hence, the sub–path from Q to P is of type $S^+I^{L+} * ZI^{L+}_P$. Referring to the graph in Fig. 8(c), from all other points Q in Region VI the path is still of type $S^+I^{L+} * ZI^{L+}_P$. Notice that the common border of Regions VI and II_C is an optimal path of type $S^+I^{L+}_P$ as proved in Proposition 9, see Fig. 9. As a consequence, an infimum length path of type $S^+I^{L+} * ZI^{L+}_P$ can not cross that border. Hence, from those Q the path of infimum length can only cross the involute I^L_P starting from point P_5. The infimum length path from that involute are of type $S^+I^{L+} * ZI^{L+}_P$ and hence the possible concatenation with those paths is through a straight arc that hat smoothly connects Q to those paths.

Region II_C: From points Q in this region the point P can be reached through paths with last extremal S^+ or I^{L+}_P, see the borders of the adjacent regions. Referring to the graphs in Figures 8(a) and 8(c), no extremal can precede S^+ in an optimal path while only S^+ can precede I^{L+}_P. Indeed, arc I^{L+}_P is preceded by Z or by I^{R-} only for points that are outside II_C. ■

B. Optimal synthesis for P with $\rho_P > \rho_2$

We will now prove that for P with $\rho_P > \rho_2$ a new Region is obtained with respect to the case $\rho_P \leq \rho_2$ based on a similar approach to the one used in Proposition 9. For example, the circumference C_5 is still the locus of switching points between S^+ and I^{L+} but from a point P_5 that does not lay on I^L_P anymore.

Without loss of generality, consider P with $\rho_P > \rho_2$, and Q on I^L_P with $\rho_Q \geq \rho_P$. Referring to the graph in Fig. 8(b) the infimum length path can be of type $\mathscr{K} = S^+I^{L+} * Z * I^{R-}S^-$ or of type $\mathscr{P} = S^+I^{L+} * I^{R-}S^-$. Starting from point Q on the involute I^L_P, we are hence interested in comparing the length of paths $\mathscr{K}$ and $\mathscr{P}$. Notice that, the path of type I^{L+}_P from Q to P can be considered as a degenerate case of $\mathscr{K}$ and $\mathscr{P}$. Moreover, $\beta_Q = \arccos\frac{R_b}{\rho_Q} > \beta_P = \arccos\frac{R_b}{\rho_P} > \pi/4$. Based on the computation of first and second derivatives of $\mathscr{K}$ and $\mathscr{P}$, the infimum length paths are proved to depend on the positions of P and Q with respect to C_5. Hence, we start considering $\rho_P \leq \rho_5$. The lengths comparison can be summarized by the following theorem.

Theorem 6: Let P be a point with $\rho_2 < \rho_P \leq \rho_5$ and consider a point Q lying on the involute through P and such that $\rho_Q > \rho_P$. The infimum length path from Q to P is

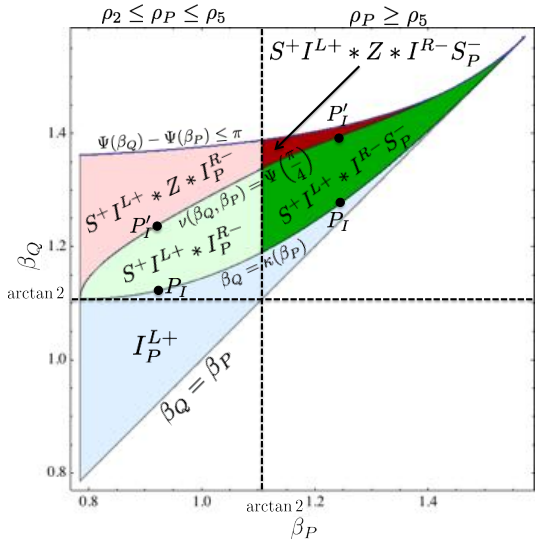

Fig. 10. Infimum length path subdivision on the (β_P, β_Q) plane with Q on I_P^L. Recall that an angle $\beta = \arctan(2)$ corresponds to a radius $\rho = \rho_5$.

1) I_P^{L+} for $\pi/4 \le \beta_P \le \beta_Q$ and $\beta_Q \le \kappa(\beta_P)$.
2) $S^+I^{L+} * I_P^{R-}$ for $\beta_Q > \kappa(\beta_P)$ and $\nu(\beta_Q,\beta_P) \le \Psi(\pi/4)$.
3) $S^+I^{L+} * Z * I_P^{R-}$ for $\beta_Q > \kappa(\beta_P)$ and $\nu(\beta_Q,\beta_P) > \Psi(\pi/4)$.

where

$$\kappa(\beta_P) = \arctan\left(\frac{1}{\cos\beta_P \sin\beta_P}\right) \tag{16}$$

and $\nu(\beta_Q,\beta_P) = \frac{1}{2}(2 - \arcsin(2\cos\beta_Q) + 2\Psi(\beta_P) - \Psi(\beta_Q))$.

For space limitations the proof of the theorem is omitted[2]. However, for reader convenience, the infimum length paths from Q on I_P^L to P are reported in the left sector of Fig. 10 as a function of $\beta_P \le \arctan(2)$ and β_Q. Referring to Figures 10 and 11, for $\rho_P \le \rho_5$, i.e. $\beta_P \le \arctan(2)$, consider all Q with $\beta_P \le \beta_Q \le \kappa(\beta_P)$. From the first case of Theorem 6, the optimal path is I_P^{L+} for all points Q on I_P^L between P and P_I characterized by $\beta_{P_I} = \kappa(\beta_P)$. Consider Q with $\kappa(\beta_P) \le \beta_Q \le \kappa(\beta_P)$ below the curve $\nu(\beta_Q,\beta_P) = \Psi(\pi/4)$. From the second case of Theorem 6 the optimal path is of type $S^+I^{L+}I_P^{R-}$ for all points Q on I_P^L between P_I and P_I' characterized by $\nu(\beta_{P_I'},\beta_P) = \Psi(\pi/4)$. Finally, consider Q above the curve $\nu(\beta_Q,\beta_P) = \Psi(\pi/4)$ with $\Psi_Q \le \pi$ (i.e. Q is on the upper half–plane). From the third case of Theorem 6 the infimum length path is of type $S^+I^{L+} * Z * I_P^{R-}$ for all points Q on I_P^L after P_I'.

From the proof of Theorem 6 in case of infimum length path of type $S^+I^{L+} * Z * I_P^{R-}$, the locus of switching points between S^+ and I^{L+} is C_5. Given P_I' the optimal path is $S^+I^{L+} * I_P^{R-}$ where the switching point between S^+ and I^{L+} is denoted by P_5, while the switching point between I^{L+} and I^{R-} is denoted by P_2. Notice that P_2 is the point of intersection between I_P^R and C_2. Hence, for all Q with infimum length path of type

[2]The complete proof of Theorems 6 and 7 and other details can be found in the Appendix of
http://www.centropiaggio.unipi.it/sites/default/files/HFOVdim.pdf

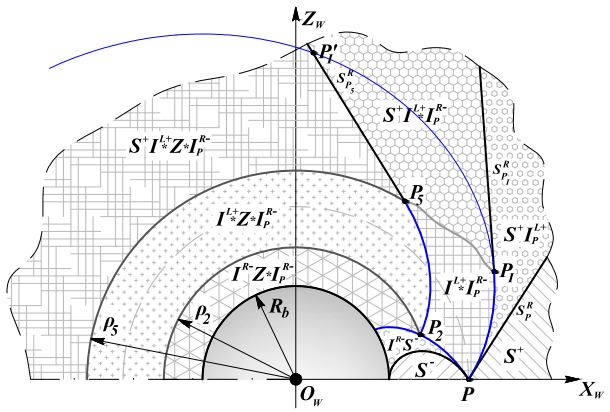

Fig. 11. Optimal synthesis with $\rho_2 < \rho_P \le R_b\sqrt{5}$.

$S^+I^{L+} * Z * I_P^{R-}$, the switching point between Z and I_P^{R-} is P_2 that is independent from Q.

The construction of Theorem 6 identifies two regions of the upper half–plane. The first region, R_1, is delimited by the circumference C_{R_b} and the arc I_P^L while the second, R_2, is the complementary one. From the analysis in Theorem 6 the optimal synthesis for $\rho_P \le \rho_5$ can be obtained straightforwardly. Indeed, for any point $Q' \in R_1$ that lays outside C_2 there exists a point Q on I_P^L such that the infimum length path from Q to P crosses Q'. For all $Q \in R_1$ inside C_2 the synthesis for $\rho_P \le \rho_2$ can be used by switching the roles of P and Q. Moreover, from the graph reported in Fig. 8(b), the only possible way to obtain an infimum length path from points $Q \in R_2$ is to connect to the path of infimum length from point on I_P^L smoothly with an arc S^+ or to go toward P directly with S^+. Finally, for the remaining points Q in the region delimited by I_P^R from P to C_{R_b} and C_{R_b} previous result can be applied by switching the roles of P and Q.

To conclude, the obtained synthesis is reported in Fig. 11. Notice that, for $\rho_P \le \rho_2$, whose synthesis is reported in Fig. 9, the points P_5, P_I and P_I' were coincident. Hence, for $\rho_2 \le \rho_P \le \rho_5$ the synthesis is similar to the one for $\rho_P \le \rho_2$ but has two more regions. However, for space limitation is not possible to provide here an analytical characterization of the curve between P_I and P_5 of switching points between S^+ and I^{L+}. Numerically, it can be obtained as a solution of a set of nonlinear equations.

To conclude the optimal synthesis analysis, the case $\rho_P > \rho_5$ must now be taken into account. Similarly to what has been done for $\rho_P \le \rho_5$ the following theorem summarizes the lengths comparison of paths $\mathscr{K}$ and $\mathscr{P}$.

Theorem 7: Let P be a point with $\rho_P > \rho_5$ and consider a point Q lying on the involute through P and such that $\rho_Q > \rho_P$. The infimum length path from Q to P is

1) I_P^{L+} for $\pi/4 \le \beta_P \le \beta_Q$ and $\beta_Q \le \kappa(\beta_P)$.
2) $S^+I^{L+} * I^{R-} S_P^-$ for $\beta_Q > \kappa(\beta_P)$ and $\nu(\beta_Q,\beta_P) \le \Psi(\pi/4)$.
3) $S^+I^{L+} * Z * I^{R-} S_P^-$ for $\beta_Q > \kappa(\beta_P)$ and $\nu(\beta_Q,\beta_P) > \Psi(\pi/4)$.

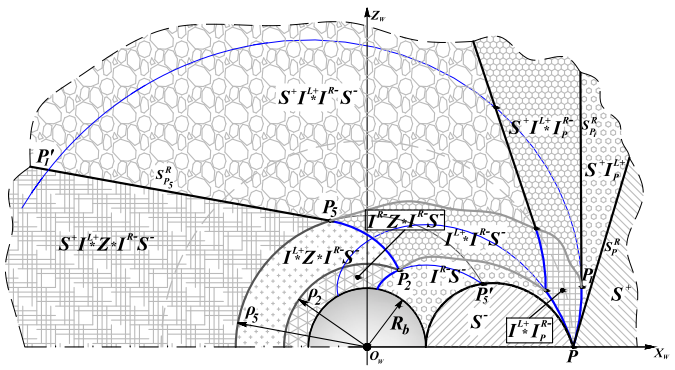

Fig. 12. Optimal synthesis with $\rho_P > R_b\sqrt{5}$.

where

$$\kappa(\beta_P) = \arctan\left(\frac{1}{\cos\beta_P \sin\beta_P}\right) \tag{17}$$

and

$$\nu(\beta_Q,\beta_P) = \frac{4 - \arcsin(2\cos\beta_Q) - \arcsin(2\cos\beta_P) + \Psi(\beta_P) - \Psi(\beta_Q)}{2}.$$

For the proof of the theorem see footnote 2. For reader convenience, the infimum length paths from Q on I^L_P to P are reported in Fig. 10 as a function of β_P and β_Q.

With respect to the analysis for $\rho_P \leq \rho_5$ the point $P_I\prime$ is such that $\nu(\beta_{P_I'},\beta_P) = \Psi(\pi/4)$ with function ν as defined in Theorem 7. From P_I' the optimal path is of type $S^+I^{L+}*I^{R-}S^-$ where the switching point between S^+ and I^{L+} is denoted by P_5 on C_5 and the switching point between I^{L+} and I^{R-} is denoted by P_2 on C_2. Finally, the switching point between I^{R-} and S^- is denoted by $P_5' \in Lim^R_P \cap C_5$.

The optimal synthesis can be obtained straightforwardly using an approach similar to the one used for $\rho_P \leq \rho_5$ and it is reported in Fig. 12. In this case, the region characterized by the optimal path of type $S^+I^{L+}*I^{R-}S^-$ formally consists in two sub regions characterized by non degenerate path of type $S^+I^{L+}*I^{R-}S^-$ and the degenerate paths of type $S^+I^{L+}*I^{R-}$.

Formally, the three synthesis obtained in this paper provide paths of infimum length that do not exist. However, by substituting the (non existing) arc Z with Z_ε an ε–optimal synthesis has been obtained such that each ε–optimal path is not longer than ε with respect to the associated infimum length path.

VII. Conclusions and Future Works

Given the finite optimal language associated to the extremals of the considered optimal control problem, all regions of points from which the optimal path does not exist have been herein characterized. However, the infimum length of paths from such regions is finite and can be analytically obtained. Its length can be used to compute an optimal synthesis of infimum length paths. Moreover, since the infimum can be arbitrarily well approximated using paths containing a finite number of switching between involute arcs the ε–optimal synthesis can be straightforwardly obtained. Notice that the ε–optimal paths can be determined based on the motor characteristics of the robotic vehicle and hence there exist control laws that are able to steer the vehicle along such paths.

Future works will be dedicated to the integration of the results obtained for the H–FOV and the V–FOV in a complete synthesis for a more realistic camera. Moreover, from such synthesis optimal feedback control laws could be determined with a similar approach to the one used in [20].

References

[1] J.-B. Hayet, "Shortest length paths for a differential drive robot keeping a set of landmarks in sight," *Journal of Intelligent & Robotic Systems*, vol. 66, no. 1-2, pp. 57–74, 2012.

[2] L. E. Dubins, "On curves of minimal length with a constraint on average curvature, and with prescribed initial and terminal positions and tangents," *American Journal of Mathematics*, vol. 79, no. 3, pp. 457–516, 1957.

[3] X. Bui, P. Souères, J.-D. Boissonnat, and J.-P. Laumond, "Shortest path synthesis for Dubins non–holonomic robots," in *Proceedings of the IEEE International Conference on Robotics and Automation*, vol. 1, 1994, pp. 2–7.

[4] J. A. Reeds and L. A. Shepp, "Optimal paths for a car that goes both forwards and backwards," *Pacific Journal of Mathematics*, vol. 145, no. 2, pp. 367–393, 1990.

[5] H. Sussmann and G. Tang, "Shortest paths for the reeds-shepp car: A worked out example of the use of geometric techniques in nonlinear optimal control," Department of Mathematics, Rutgers University, Tech. Rep., 1991.

[6] H. Souères and J. P. Laumond, "Shortest paths synthesis for a car-like robot," *IEEE Transaction on Automatic Control*, vol. 41, no. 5, pp. 672–688, May 1996.

[7] D. Balkcom and M. Mason, "Time-optimal trajectories for an omni-directional vehicle," *The International Journal of Robotics Research*, vol. 25, no. 10, pp. 985–999, 2006.

[8] H. Wang, Y. Chan, and P. Souères, "A geometric algorithm to compute time-optimal trajectories for a bidirectional steered robot," *IEEE Transaction on Robotics*, vol. 25, no. 2, pp. 399–413, 2009.

[9] H. Chitsaz, S. M. LaValle, D. J. Balkcom, and M. Mason, "Minimum wheel-rotation for differential-drive mobile robots," *The International Journal of Robotics Research*, vol. 28, no. 1, pp. 66–80, 2009.

[10] G. López-Nicolás, C. Sagüés, J. Guerrero, D. Kragic, and P. Jensfelt, "Switching visual control based on epipoles for mobile robots," *Robotics and Autonomous Systems*, vol. 56, no. 7, pp. 592 – 603, 2008.

[11] X. Zhang, Y. Fang, and X. Liu, "Visual servoing of nonholonomic mobile robots based on a new motion estimation technique," in *Proceedings of the 48th IEEE Conference on Decision and Control and 28th Chinese Control Conference.*, 2009, pp. 8428 –8433.

[12] D. Panagou and V. Kumar, "Maintaining visibility for leader-follower formations in obstacle environments," in *Proceedings of the IEEE International Conference on Robotics and Automation*, 2012, pp. 1811–1816.

[13] P. Murrieri, D. Fontanelli, and A. Bicchi, "A hybrid-control approach to the parking problem of a wheeled vehicle using limited view-angle visual feedback," *Int. Jour. of Robotics Research*, vol. 23, no. 4–5, pp. 437–448, April 2004.

[14] N. Gans and S. Hutchinson, "Stable visual servoing through hybrid switched system control," *IEEE Transactions on Robotics*, vol. 23, no. 3, pp. 530–540, June 2007.

[15] ——, "A stable vision-based control scheme for nonholonomic vehicles to keep a landmark in the field of view," in *Proceedings of the IEEE International Conference on Robotics and Automation*, 2007, pp. 2196 –2201.

[16] J.-B. Hayet, H. Carlos, C. Esteves, and R. Murrieta-Cid, "Motion planning for maintaining landmarks visibility with a differential drive robot," *Robotics and Autonomous Systems*, vol. 62, no. 4, pp. 456 – 473, 2014.

[17] J.-B. Hayet, C. Esteves, G. Arechavaleta, O. Stasse, and E. Yoshida, "Humanoid locomotion planning for visually-guided tasks," *International Journal of Humanoid Robotics*, vol. 9, no. 2, 2012.

[18] P. Salaris, D. Fontanelli, L. Pallottino, and A. Bicchi, "Shortest paths for a robot with nonholonomic and field-of-view constraints," *IEEE Transactions on Robotics*, vol. 26, no. 2, pp. 269–281, April 2010.

[19] P. Salaris, L. Pallottino, and A. Bicchi, "Shortest paths for finned, winged, legged, and wheeled vehicles with side-looking sensors," *The International Journal of Robotics Research*, vol. 31, no. 8, pp. 997–1017, 2012.

[20] P. Salaris, L. Pallottino, S. Hutchinson, and A. Bicchi, "From optimal planning to visual servoing with limited fov," in *Proceedings of the IEEE/RSJ International Conference on Intelligent Robots and Systems*, 2011, pp. 2817–2824.

[21] G. López-Nicolás, S. Bhattacharya, J. Guerrero, C. Sagüés, and S. Hutchinson, "Switched homography-based visual control of differential drive vehicles with field-of-view constraints," in *Proceedings of the IEEE International Conference on Robotics and Automation*, 2007, pp. 4238–4244.

[22] P. Salaris, A. Cristofaro, L. Pallottino, and A. Bicchi, "Shortest paths for wheeled robots with limited field-of-view: introducing the vertical constraint," in *Proceedings of the 52nd IEEE Conference on Decision and Control*, 2013, pp. 5143–5149.

[23] R. Hartley and A. Zisserman, *Multiple View Geometry in Computer Vision*. Cambridge University Press, 2003.

[24] A. Bryson and Y. Ho, *Applied optimal control*. Wiley New York, 1975.

[25] E. H. Lockwood, *"The Limaçon." Ch. 5 in A Book of Curves*. Cambridge, England: Cambridge University Press, 1967, pp. 44–51.

[26] P. Salaris, F. Belo, D. Fontanelli, L. Greco, and A. Bicchi, "Optimal paths in a constrained image plane for purely image-based parking," in *Proceedings of the IEEE/RSJ International Conference on Intelligent Robots and Systems*, 2008, pp. 1673–1680.

APPENDIX

A. Proof of Proposition 2

Proposition 2: For any starting point Q, all points of Lim_Q (Λ_Q) are reachable by a forward (backward) straight path without violating the V–FOV constraints.

The proof of Proposition 2, is based on how the projection on the image plane of the landmark moves within the sensor limits (see [26]) when vehicle performs extremal maneuvers. For this purposes, we need to introduce the basic notations and results of the projective geometry used in visual servoing applications. Let $F = ({}^I x, {}^I y)$ be the position of the landmark with respect to a reference frame $\langle I \rangle = (O_I, X_I, Y_I)$ centered on the principal point of the image plane (see Fig. 2). The velocity of F is related to the linear and angular velocity (v and ω) of the vehicle through the image Jacobian [23]. For a rotation on the spot ($*$), setting $v = 0$ in the image Jacobian, the trajectories follows by F is given by

$$ {}^I y = \frac{{}^I y_i \cos\left(\arctan\left(\frac{{}^I x_i}{f}\right)\right)}{\cos\left(\arctan\left(\frac{{}^I x}{f}\right)\right)} = \frac{{}^I y_i \cos\beta_i}{\cos\beta} \tag{18} $$

where $({}^I x_i, {}^I y_i)$ is the initial position of F with respect to $\langle I \rangle$. Equation (18) represents a conic, i.e. the intersection between the image plane and the right circular cone with vertex in O_c and directrix passing through the landmark position. For a straight lines path (S), setting $\omega = 0$ in the image Jacobian, the trajectory follows by F is given by

$$ {}^I y = \frac{{}^I y_i}{{}^I x_i} {}^I x \tag{19} $$

which represents a straight line passing through O_I.

With those notations and results we can prove Proposition 2.

Proof: For any starting point $Q = (\rho_Q, \psi_Q)$, with $\beta_Q = 0$, let us consider the vehicle rotating on the spot. During such maneuver, the landmark moves on the image plane along a conic until the V–FOV constraint is activated and ${}^I y = f \tan\hat{\phi}$. Let $\tilde{\beta}$ be the corresponding value of the bearing angle. The new direction of motion of the vehicle is now tangent to an involute of circle. Moreover, from (5), $\rho_Q \cos\tilde{\beta} = \frac{h}{\tan\hat{\phi}} = R_b$. From all configurations $(\rho_Q, \psi_Q, \beta_Q)$ with $\beta_Q \in [-\tilde{\beta}, \tilde{\beta}]$ the vehicle can move backward on a straight line without violating the constraint. Hence, referring to Definition 4, the region of points reachable from Q with a backward straight line is Λ_Q.

In order to determine the region reachable with a forward straight line, assume $\eta_Q = (\rho_Q, \psi_Q, \beta_Q)$ with bearing angle $\beta_Q \in]-\tilde{\beta}, \tilde{\beta}[$, i.e. the direction of motion is not necessarily tangent to one of the involutes through Q. Let V be the point on the forward straight line where the V–FOV constraint is activated. While the vehicle moves along the straight line, the landmark moves, in the image plane, along a straight line as well, i.e. from (4) and (5), ${}^I y = \frac{{}^I y_i}{{}^I x_i} {}^I x$ where ${}^I y_i = f \frac{h}{\rho_Q \cos\beta_Q}$ and ${}^I x_i = f \tan\beta_Q$. As before, when the V–FOV constraint is active, ${}^I y = f \tan\hat{\phi}$ and hence ${}^I x = f \frac{\rho_Q}{h} \tan\hat{\phi} \sin\beta_Q$. From (4), in V, ${}^I x = f \tan\beta_V$ and hence the bearing angle in V is $\beta_V = \arctan\left(\frac{\rho_Q}{h} \tan\hat{\phi} \sin\beta_Q\right) = \bar{\beta}$. Moreover, since the V–FOV constraint is active in V, the direction of motion of the vehicle is tangent to an involute through V. Hence, the distance ρ_V can be determined by the equation $\rho_V \cos\beta_V = R_b$. By using the Carnot theorem and $R_b = \frac{h}{\tan\hat{\phi}}$, distance d covered by the vehicle is $d = a + b\cos\beta$ with $a = -R_b$ and $b = \rho_Q > a$, i.e. the equation describing a Pascal's Limaçon with respect to a reference frame with origin in Q and the x-axis aligned with the line through O_w and Q, (see Fig. 4). As a consequence, referring to Definition 3, points of Lim_Q are reachable by a forward straight line. ■

B. Proof of Proposition 4

Consider $Q_1 = (\rho_{Q_1}, \psi_{Q_1})$ and $Q_2 = (\rho_{Q_2}, \psi_{Q_2})$ with $\rho_{Q_1} = \rho_{Q_2}$ and $\psi_{Q_1} > \psi_{Q_2}$. The points Q_1 and Q_2 can be connected by two paths, each one symmetric with respect to the bisectrix of angle $\widehat{Q_1 O_w Q_2}$, consisting of two pairs of involute curves $\mathscr{C}_1 = I^{L+} * I^{R-}$ and $\mathscr{C}_2 = I^{R-} * I^{L+}$. Let $H_1 = (\rho_{H_1}, \psi_{H_1})$ and $H_2 = (\rho_{H_2}, \psi_{H_2})$ be the points of intersection of the involute curves on $\mathscr{C}_1$ and $\mathscr{C}_2$ respectively, i.e. $\rho_{H_1} < \rho_{Q_i} < \rho_{H_2}$ and $\psi_{H_1} = \psi_{H_2}$. We denote by $L(\mathscr{C}_1)$ and $L(\mathscr{C}_2)$ the lengths of the curves $\mathscr{C}_1$ and $\mathscr{C}_2$, respectively.

Proposition 4: There exist $\bar{\rho} > \rho_2 > \tilde{\rho}$ such that

1) $\rho_{Q_1} \leq \rho_2 \Rightarrow L(\mathscr{C}_2) \leq L(\mathscr{C}_1) \; \forall \rho_{H_1}$.

2) $\rho_{Q_1} \in (\rho_2, \bar{\rho}), \rho_{H_1} < \tilde{\rho} \;\Rightarrow\; L(\mathscr{C}_2) < L(\mathscr{C}_1)$
3) $\rho_{Q_1} \in (\rho_2, \bar{\rho}), \rho_{H_1} > \tilde{\rho} \;\Rightarrow\; L(\mathscr{C}_1) < L(\mathscr{C}_2)$
4) $\rho_{Q_1} \geq \bar{\rho} \;\Rightarrow\; L(\mathscr{C}_1) \leq L(\mathscr{C}_2)\ \forall \rho_{H_1}$.

Proof: Consider the parametric equations of involute I_0

$$\begin{cases} x(\lambda) = R_b(\cos\lambda + \lambda\sin\lambda) \\ z(\lambda) = R_b(\sin\lambda - \lambda\cos\lambda) \\ \lambda = \tan\beta,\ \beta \geq 0. \end{cases}$$

Since the involute length depends on the cosine of angle β, without loss of generality we consider $H_2' = (\rho_{H_2}, \psi_{H_2'})$ that lays on I_0 as Q_1 and H_1 and has $\beta_{H_2'} = -\beta_{H_2}$, see Fig. 3.

The heading angles corresponding to the points Q_1, H_1 are given by

$$\beta_{Q_1} = \arccos\left(\frac{R_b}{\rho_{Q_1}}\right) = \arctan\sqrt{\frac{\rho_{Q_1}^2}{R_b^2} - 1}, \tag{20}$$

$$\beta_{H_1} = \arccos\left(\frac{R_b}{\rho_{H_1}}\right) = \arctan\sqrt{\frac{\rho_{H_1}^2}{R_b^2} - 1}. \tag{21}$$

The heading angle associated to H_2' can be computed by means of the function $\Psi(\beta)$, imposing the identity $\psi_{H_1} = \psi_{H_2}$, $\beta_{H_2'} = \Psi^{-1}(2\Psi(\beta_{Q_1}) - \Psi(\beta_{H_1}))$. In this way one has

$$\begin{array}{l} L(\mathscr{C}_1)/2 = \ell_1(\beta_{Q_1}, \beta_{H_1}) = \ell_0(\beta_{Q_1}) - \ell_0(\beta_{H_1}) \\ L(\mathscr{C}_2)/2 = \ell_2(\beta_{Q_1}, \beta_{H_2}) = \ell_0(\beta_{H_2'}) - \ell_0(\beta_{Q_1}) \end{array} \tag{22}$$

To simplify the notation, let $y = \beta_{H_1} \leq w = \beta_{Q_1} \leq y' = \beta_{H_2'}$. To compare $L(\mathscr{C}_1)$, $L(\mathscr{C}_2)$ we analyze the function

$$\Delta_\ell(w,y) = \ell_2(w, y'(y)) - \ell_1(w,y) = \ell_0(y) + \ell_0(y'(y)) - 2\ell_0(w), \tag{23}$$

where $y'(y) = \Psi^{-1}(2\Psi(w) - \Psi(y))$. The function $\Delta_\ell(w,y)$ is always zero for $y = w$, i.e. $\Delta_\ell(w,w) = 0$ $w \in [0, \pi/2]$. Moreover we will now prove that it is always negative and increasing if $w \leq \pi/4$ while, for $w > \pi/4$ it is negative for $y \leq \bar{y} \leq \pi/4$ and positive for $y \in [\bar{y}, w]$ (where $\bar{y}$ will be determined in the following). To prove this we analyze the sign of the derivative of $\Delta(w,y)$ with respect to y.

The derivate of $y'(y)$ with respect to y is $\frac{dy'(y)}{dy} = -\frac{\tan^2 y}{\tan^2 y'(y)}$. For the sake of simplicity, in the following, we omit the dependency of y in $y'(y)$. Hence,

$$\frac{\partial \Delta_\ell(w,y)}{\partial y} = \frac{d\ell_0(y)}{dy} - \frac{d\ell_0(y')}{dy}\frac{\tan^2 y}{\tan^2 y'}.$$

Substituting $\frac{d\ell_0(y)}{dy} = \frac{R_b}{2}(1 + \tan^2 y)$ we obtain

$$\frac{\partial \Delta_\ell(w,y)}{\partial y} = R_b \frac{\tan y}{\tan y'}(\tan y' - \tan y)(1 - \tan y' \tan y).$$

Since $y \leq w \leq y'$ we have that the sign of $\frac{\partial \Delta_\ell(w,y)}{\partial y}$ is equal to the sign of the function $F(y) = 1 - \tan y' \tan y$ with $y \in [0, w]$.

Upon simple computations we obtain

$$\frac{dF(y)}{dy} = -\frac{\tan y' - \tan y}{\tan^2 y'}(\tan^2 y + \tan^2 y' + \tan y' \tan y + \tan^2 y' \tan^2 y),$$

that is always negative for $y \in [0, w)$ and zero only in $y = w$. Moreover, $F(0) = 1$ and $F(w) = 1 - \tan^2 w$. Hence, $F(y)$ is always non-negative for $w \leq \pi/4$ (is zero only for $y = w = \pi/4$) while is positive and then negative for $\pi/4 \leq w \leq \bar{w}$ and finally always positive for $w > \bar{w}$. The value $\bar{\rho}$ associated to $\beta_{Q_1} = \bar{w}$ is hence larger than ρ_2, i.e. $\bar{\rho} > \rho_2$.

Based on those results, we have that $\Delta_\ell(w,y)$ is always negative and increasing ($F(y)$ is non-negative) if $w = \beta_{Q_1} \leq \pi/4$ (i.e. $\rho_{Q_1} \leq \rho_2$) while, for $\pi/4 < w \leq \bar{w}$ (i.e. $\rho_2 \leq \rho_{Q_1} \leq \bar{\rho}$) there exists a $\tilde{y} \leq \pi/4$ (i.e. a $\tilde{\rho} \leq \rho_2$) such that $\Delta_\ell(w,y)$ is negative for $y = \beta_{H_1} < \tilde{y}$ (i.e. $\rho_{H_1} < \tilde{\rho}$) and positive for $y \in [\tilde{y}, w]$ (i.e. $\rho_{H_1} \geq \tilde{\rho}$), finally for $w > \bar{w}$ (i.e. $\rho_{Q_1} > \bar{\rho}$) is always positive. ∎

C. Proof of Corollary 1

Corollary 1: Given a trajectory $C^{(n)}$ from Q_1 to Q_2 on the circumference of radius ρ_2 consisting of n identical sub–paths of type $\mathscr{C}_2$ and a positive parameter $\varepsilon > 0$, given

$$n \geq \frac{c_0(\psi_{Q_1} - \psi_{Q_2})^2}{2\varepsilon}.$$

we have

$$L(C^{(n)}) - L_{inf}(Q_1, Q_2) \leq \varepsilon.$$

Proof: Since $\Psi(\pi/4 + s) \geq \Psi(\pi/4) + s\ \forall s \in \left[0, \frac{\pi}{4}\right)$, and since the function Ψ^{-1} is increasing, the following inequality can be deduced

$$\Psi^{-1}(\Psi(\pi/4) + s) \leq \pi/4 + s \quad \forall s \in \left[0, \frac{\pi}{4}\right).$$

Moreover, the single pair of involute of type $\mathscr{C}_2$ between Q_1 and Q_2 with $\widehat{Q_2 O_w Q_1} = \zeta$ has length:

$$L(\mathscr{C}_2) = L(C^{(1)}) = 2\left(\ell_0\left(\Psi^{-1}\left(\frac{\zeta}{2} + \Psi(\pi/4)\right)\right) - \ell_0(\pi/4)\right).$$

Hence,

$$\begin{aligned} L(C^{(n)}) &= 2n\left(\ell_0\left(\Psi^{-1}\left(\frac{\zeta}{2n} + \Psi(\pi/4)\right)\right) - \ell_0(\pi/4)\right) \leq \\ &\leq 2n\left(\ell_0\left(\pi/4 + \frac{\zeta}{2n}\right) - \ell_0(\pi/4)\right). \end{aligned}$$

The following estimate holds

$$\ell_0(\pi/4 + s) \leq \ell_0(\pi/4) + 2R_b s + c_0 s^2, \tag{24}$$

with $c_0 > 4R_b$ and $s \in [0, f(c_0))$ where $f(c_0)$ is solution of (24) as an equality. Since we are interested in finding a good approximation of the shortest path, it is reasonable to consider small increments of the variable $\zeta/n \leq f(c_0)$. Substituting (24) in $L(C^{(n)})$, we obtain $L(C^{(n)}) \leq 2R_b\zeta + c_0\frac{\zeta^2}{n} \quad \forall n \geq 2$, or equivalently

$$L(C^{(n)}) - L_{inf}(Q_1, Q_2) \leq c_0\frac{\zeta^2}{n} \quad \forall n \geq 2.$$

As a consequence the bound $L(C^{(n)}) - L_{inf}(Q_1, Q_2) \leq \varepsilon$ is ensured if

$$n \geq \frac{c_0(\psi_{Q_1} - \psi_{Q_2})^2}{2\varepsilon}.$$

∎

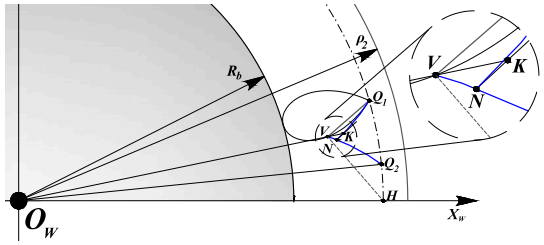

Fig. 13. Graphical construction for the proof of Proposition 6.

D. Proof of Proposition 6

For the proof of Proposition 6 we first need the following:

Lemma 1: Consider a function $f(x)$ with $f(0)=0$, $f(\bar{x})>0$, $f'(x)\geq 0$ for $x\in[0,\bar{x}]$ with $\bar{x}\leq 1$ and a function $g(x)$ with $g(\bar{x})=f(\bar{x})>0$, $g(1)=0$ and $g'(x)\leq 0$ for $x\in[\bar{x},1]$. Let L_f and L_g be the lengths of the paths $\gamma_f(s)=f(s\bar{x})$ and $\gamma_g(s)=g(s(1-\bar{x})+\bar{x})$ with $s\in[0,1]$ respectively. The following holds

$$L_f\leq 1+L_g.$$

Proof: Since for $x,y\geq 0$, $\sqrt{x+y}\leq\sqrt{x}+\sqrt{y}$, the length of the path $\gamma_f(s)$ verifies

$$L_f=\int_0^{\bar{x}}\sqrt{1+f'^2(s)}ds\leq\int_0^{\bar{x}}(1+f'(s))ds=\bar{x}+f(\bar{x}).$$

On the other hand, since $g'(x)\leq 0$, the length of the path $\gamma_g(s)$ verifies

$$L_g=\int_{\bar{x}}^1\sqrt{1+g'^2(s)}ds\geq-\int_{\bar{x}}^1 g'(s)ds=g(\bar{x})-g(1)=f(\bar{x}).$$

Hence, $L_f\leq\bar{x}+f(\bar{x})\leq 1+f(\bar{x})=1+L_g$. ■

Proposition 6: Any path of type S^+*I^{R-} or $I^{L+}*S^-$ can be shortened by a path of type $S^+I^{L+}*I^{R-}S^-$ or $S^+I^{L+}*Z*I^{R-}S^-$.

Proof: Consider a path of type S^+*I^{R-} and assume that it evolves completely outside C_2 . There always exist two points Q_1 and Q_2 along arcs S^+ and I^{R-} respectively, with $\rho_{Q_1}=\rho_{Q_2}>\rho_2$.

We now prove that the subpath $S^+_{Q_1}*I^{R-}_{Q_2}$ can be shortened by paths of type $I^{L+}_{Q_1}*I^{R-}_{Q_2}$, $S^+_{Q_1}I^{L+}*I^{R-}_{Q_2}$ or $S^+_{Q_1}I^{L+}*Z*I^{R-}_{Q_2}$. Indeed, consider the two palindrome paths constructed from $S^+_{Q_1}*I^{R-}_{Q_2}$: $S^+_{Q_1}*I^{R-}*I^{L+}*S^-_{Q_1}$ and $I^{L+}_{Q_1}*I^{R-}_{Q_2}$. From Proposition 1, those paths are of smaller or of equal length with respect to $S^+_{Q_1}*I^{R-}_{Q_2}$. If $I^{L+}_{Q_1}*I^{R-}_{Q_2}$ is smaller the thesis is proved. Otherwise, since the path $S^+_{Q_1}*I^{R-}*I^{L+}*S^-_{Q_1}$ is assumed to evolve outside C_2, from points 3 or 4 of Proposition 4 and point 2 of Theorem 2, the subpath $I^{R-}*I^{L+}$ can be shortened by $I^{L+}*I^{R-}$ or by $I^{L+}*Z*I^{R-}$. Considering again the original path S^+*I^{R-} the thesis follows from the fact that a path of type S^-*I^{R-} can be shortened by a path of type $I^{R-}S^-$, see [22].

If the path of type S^+*I^{R-} evolves also inside C_2, there always exist two points Q_1 and Q_2 along arcs S^+ and I^{R-} respectively, with $\rho_{Q_1}=\rho_{Q_2}<\rho_2$. We will prove that the path $S^+_{Q_1}*I^{R-}_{Q_2}$ is longer than the path $I^{L+}_{Q_1}*I^{R-}_{Q_2}$.

Let V and N be the switching points between $S^+_{Q_1}$ and $I^{R-}_{Q_2}$ and between $I^{L+}_{Q_1}$ and $I^{R-}_{Q_2}$, respectively. It is hence sufficient to prove that the path consisting of S^+ between Q_1 and V and of I^{R-} from V to N is longer than the arc I^{L+} between Q_1 and N. To do this, we apply Lemma 1 where $\gamma_f(s)$ is the arc I^{L+} (between Q_1 and N) and $\gamma_g(s)$ is the arc I^{R-} (between V and N). The lemma will be applied considering the origin in Q_1 and the x–axis laying along S^+. Moreover, the distances are normalized with respect to the length of the S^+ arc. Once the hypothesis of the lemma are verified the thesis of this proposition will hence follow straightforwardly.

To apply Lemma 1 we first need to prove that the projection of point N along S^+ lays between Q_1 and V, i.e. that $\bar{x}$ of the lemma lays in $[0,1]$. Secondly we need to prove that the half–line from the origin through V forms an angle with the line through Q_1 and V that is smaller with respect to the angle formed with the tangent to $I^{L+}_{Q_1}$ in V. Indeed, this would prove that $f'(x)\geq 0$. The condition $g'(x)\leq 0$ for $x\in[\bar{x},1]$ is clearly verified.

To prove that the projection of point N along S^+ lays between Q_1 and V, consider the point H of intersection between the orthogonal to S^+ through V and the circle of radius $\rho_{Q_1}=\rho_{Q_2}=\rho_{Q_H}$. We need to prove that $\widehat{VO_wH}\geq\widehat{VO_wQ_2}$. Indeed, if this holds the projection of Q_2 on S^+ lays between Q_1 and V and even more so does N.

For the relations between heading angles of points on involutes and their distance with respect to the origin, we have that the angle $\widehat{VO_wQ_2}=\Psi(\beta_{Q_1})-\Psi(\beta_V)=\tan\beta_{Q_1}-\beta_{Q_1}-(\tan\beta_V-\beta_V)$. On the other hand, for the definition of point H, the angle $\widehat{O_wVH}=\pi/2+\beta_V$ while for sine rule $\widehat{VHO_w}=\arcsin\left(\frac{\rho_V}{\rho_{Q_1}}\cos\beta_V\right)$. Since $\rho_V=\frac{R_b}{\cos\beta_V}$ and $\rho_{Q_1}=\frac{R_b}{\cos\beta_{Q_1}}$, $\widehat{VHO_w}=\arcsin\cos\beta_{Q_1}=\pi/2-\beta_{Q_1}$. Hence, from the sum of internal angles of a triangle and the fact that angles are smaller than $\pi/2$, we have $\widehat{VO_wH}=\beta_{Q_1}-\beta_V$. To conclude we have that $\widehat{VO_wH}-\widehat{VO_wQ_2}=2\beta_{Q_1}-\tan\beta_{Q_1}-(2\beta_V-\tan\beta_V)$. Since function $F(\beta)=2\beta-\tan\beta$ is increasing in $[0,\pi/4]$ and since $\beta_V<\beta_{Q_1}$ it holds $\widehat{VO_wH}-\widehat{VO_wQ_2}\geq 0$ and hence the first hypothesis of the lemma is verified.

To verify the second hypothesis let K be the point of intersection between the half–line from O_W through V and the tangent to I^{L+} in N. The hypothesis holds if $\widehat{O_WKN}>\beta_V$. The angle $\widehat{O_WNK}=\pi-\beta_N$ while $\widehat{NO_WK}=\tan\beta_N-\beta_N-(\tan\beta_V-\beta_V)$. Hence, $\widehat{O_WKN}=2\beta_N-\tan\beta_N-(\beta_V-\tan\beta_V)$. Since $\beta_N>\beta_V$ and the function $F(\beta)$ is increasing we have $\widehat{O_WKN}>\beta_V$ and hence the thesis.

A similar proof can be applied to paths of type $I^{L+}*S^-$. ■

E. Proof of Theorem 4

Theorem 4: Given the initial point $Q=(\rho_Q,\psi_Q)$, the final point $P=(\rho_P,0)$ and the circumference C_2 of radius ρ_2, the optimal language $\mathscr{L}_O$ is characterized as follows:

a) For $\rho_Q,\rho_P\leq\rho_2$ the infimum length paths are of type S^+I^{L+}, $I^{R-}S^-$, $I^{R-}*I^{L+}$ or $I^{R-}Z*I^{L+}$ (or degenerate cases).

b) For $\rho_Q,\rho_P\geq\rho_2$ the infimum length paths are of type $S^+I^{L+}*I^{R-}S^-$ or $S^+I^{L+}*Z*I^{R-}S^-$ (or degenerate cases).

c) For $\rho_P \leq \rho_2 \leq \rho_Q$ the infimum length paths are of type S^+I^{L+} or $S^+I^{L+} * ZI^{L+}$ (or degenerate cases).
d) For $\rho_Q \leq \rho_2 \leq \rho_P$ the infimum length paths are of type $I^{R-}S^-$ or $I^{R-}Z * I^{R-}S^-$ (or degenerate cases).

Proof:

a) For Q and P with $\rho_Q, \rho_P \leq \rho_2$, the sub–path of type $\mathscr{C}_1 = I^{L+} * I^{R-}$ does not belong to an infimum length path. Indeed, if it does there exists a pair of points Q_1 and Q_2 with $\rho_{Q_1} = \rho_{Q_2} \leq \rho_2$, i.e. that verifies the first condition of Proposition 4, for which $\mathscr{C}_2$ is shorter than $\mathscr{C}_1$.
Moreover, from Theorem 3, the infimum length path from Q to P lays completely inside the circumference C_2 or, at most, contains the sub–path Z. Hence, the sequences $Z * I^{R-}$ and $I^{L+} * Z$, as $\rho_Q \leq \rho_2$, can not be part of an infimum length path. Hence, the sufficient optimal language is described by the graph represented in Fig. 8(a).
b) For $\rho_Q, \rho_P \geq \rho_2$, from cases 3) and 4) of Proposition 4 and from the case 2) of the same proposition and Theorem 3, the infimum length path from Q to P can not include a sub–path of type $\mathscr{C}_2 = I^{R-} * I^{L+}$. Indeed, if $\rho_Q, \rho_P \geq \rho_2$ one of the conditions 2)–4) of Proposition 4 holds. In cases 3) and 4) the sub–path $\mathscr{C}_2$ can be shortened by $\mathscr{C}_1$. On the other hand, in case 2), by applying Theorem 3 the sub–path $\mathscr{C}_2$ can be shortened by a path of type $I^{L+} * Z * I^{R-}$.
Moreover, similarly to the previous case, the infimum length path from Q to P lays completely outside the circumference C_2 or, at most, contains the sub–path Z. Hence, $Z * I^{L+}$ and $I^{R-} * Z$ can not be part of an infimum length path. Concluding, the sufficient optimal language is described by the graph represented in Fig. 8(b).
c) For $\rho_P \leq \rho_2 \leq \rho_Q$ there always exists a point V on the infimum length path that lays on C_2. The sub–path from V to P has been previously considered in point a) ($\rho_V, \rho_P \leq \rho_2$). Hence, from the graph in Fig. 8(a) the only infimum length sub–path is of type ZI^{L+}. On the other hand, the sub–path from Q to V has been considered in point b) ($\rho_V, \rho_Q \geq \rho_2$). Hence, from the graph in Fig. 8(b), to reach Z, the infimum length sub–path is of type $S^+I^{L+} * Z$ or of type $S^+ * S^-$. The sufficient optimal language is finally described by the graph represented in Fig. 8(c).
d) Same reasoning used in c), switching the roles of P and Q, can be done for $\rho_Q \leq \rho_2 \leq \rho_P$ leading to the sufficient optimal language described in Fig. 8(d). Notice that the switch between I^{R-} (I^{L+}) and Z may occur only once in any infimum length path.

■

Paolo Salaris Paolo Salaris received the "Laurea" in Electrical Engineering in 2007 and the Doctoral degree in Robotics, Automation and Bioengineering in 2011 at the Research Center "E.Piaggio" of the University of Pisa. He has been Visiting Scholar at Beckman Institute for Advanced Science and Technology, University of Illinois, Urbana-Champaign in 2009. He has been a PostDoc at the Research Center "E.Piaggio" from 2011 to 2013 and currently is a PostDoc at LAAS-CNRS in Toulouse. His main research interests within Robotics are in optimal motion planning, control for nonholonomic vehicles, visual servo control and motion segmentation and generation for humanoid robots.

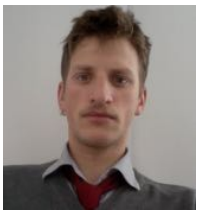

Andrea Cristofaro has received the M.Sc. in Mathematics from University of Rome La Sapienza (Italy) in 2005 and the PhD in Information Science and Complex Systems from University of Camerino (Italy) in 2010. Between 2010 and 2013 he has been first with eMotion research team, INRIA Rhone-Alpes, Grenoble (France) and then with Department of Mathematics, University of Camerino (Italy). He is currently a post-doc researcher at the Department of Engineering Cybernetics, Norwegian University of Science and Technology and Center for Autonomous Marine Operations and Systems (AMOS), Trondheim (Norway). His research interests include: constrained and robust control, filtering and estimation methods, optimization, control allocation, autonomous vehicles, control of partial differential equations.

Lucia Pallottino received the "Laurea" degree in Mathematics from the University of Pisa in 1996, and the Ph.D. degree in Robotics and Industrial Automation degree from the University of Pisa in 2002. She has been Visiting Scholar in the Laboratory for Information and Decision Systems at MIT, Cambridge, MA and Visiting Researcher in the Mechanical and Aerospace Engineering Department at UCLA, Los Angeles, CA. She joined the Faculty of Engineering in the University of Pisa as an Assistant Professor in 2007. Her main research interests within Robotics are in optimal motion planning and control, multi-agent systems and cooperating objects.

Antonio Bicchi is Professor of Robotics at the University of Pisa, and Senior Scientist at the Italian Institute of Technology in Genoa. He graduated from the University of Bologna in 1988 and was a postdoc scholar at M.I.T. Artificial Intelligence lab in 19881990. He leads the Robotics group at the Research Center "E. Piaggio" of the University of Pisa since 1990, and served as Director from 2003 to 2012. He is an Adjunct Professor at the School of Biological and Health Systems Engineering of Arizona State University since 2013. He is Editor-in-Chief for the book series "Springer Briefs on Control, Automation and Robotics," and is in the editorial board of several scientific journals. His main research interests are in Robotics, Haptics, and Control Systems in general. He has published more than 300 papers on international journals, books, and refereed conferences.